Finding Near-Optimal Configurations in Colossal Spaces with Statistical Guarantees

JEHO OH and DON BATORY, The University of Texas at Austin
RUBÉN HERADIO, Universidad Nacional de Educación a Distancia

A *Software Product Line* (SPL) is a family of similar programs. Each program is defined by a unique set of features, called a *configuration*, that satisfies all feature constraints. "What configuration achieves the best performance for a given workload?" is the SPL *Optimization* (SPLO) challenge. SPLO is daunting: just 80 unconstrained features yields 10^{24} unique configurations, which equals the estimated number of stars in the universe. We explain (a) how uniform random sampling and random search algorithms solve SPLO more efficiently and accurately than current machine-learned performance models, and (b) how to compute statistical guarantees on the quality of a returned configuration, *i.e.,* it is within x% of optimal with y% confidence.

Additional Key Words and Phrases: software product lines, configuration optimization, product spaces, machine learning, uniform random sampling, random search, order statistics

ACM Reference format:
Jeho Oh, Don Batory, and Rubén Heradio. 2022. Finding Near-Optimal Configurations in Colossal Spaces with Statistical Guarantees. *ACM Trans. Softw. Eng. Methodol.* 1, 1, Article 1 (September 2022), 36 pages.
https://doi.org/10.1145/nnnnnnn.nnnnnnn

1 INTRODUCTION

[1] A *Software Product Line* (SPL) is a family of programs with similar functionalities. Each SPL program or *product* is defined by *features*, *i.e.,* standardized increments of program functionality. Features have constraints: a feature may require and/or preclude other features. All features and their constraints are defined in a *feature model*. A *configuration* is a unique set of features that satisfies the SPL's feature model. The *configuration space* or *product space* of an SPL, denoted $\mathbb{C}$, is the set of all SPL configurations, exactly one program/product per configuration. A configuration space can be *colossal* ($\gg 10^{10}$); a set of f unconstrained features yields a space of size 2^f. A space of size 250K, which is near the upper-limit to product space enumeration [116], has $f \approx 18$ features, which is tiny for an SPL. Most SPLs are larger. Table 1 lists the sizes of contemporary SPLs taken from [48, 50, 69, 79, 89].

SPL	#Features	$\lvert\mathbb{C}\rvert$
JHipster 3.6.1	45	$2.6{\cdot}10^{4}$
axTLS 1.5.3	64	$3.9{\cdot}10^{12}$
uClib-ng 1.0.29	269	$8.0{\cdot}10^{26}$
ToyBox 0.7.5	316	$1.4{\cdot}10^{81}$
BusyBox 1.23.2	613	$7.4{\cdot}10^{146}$
EmbToolKit 1.7.0	2,331	$4.0{\cdot}10^{334}$
LargeAutomotive	17,365	$5.3{\cdot}10^{1,441}$

Table 1. SPL space sizes.

Clients want an SPL program to satisfy constraints. *Functionality constraints* declare required or forbidden features. There are environmental (hardware and platform) constraints. There are performance constraints on program usage workloads. There are specification challenges: mutually

[1] This paper extends two prior publications: [91] from 2017 and [16] from 2021.

1049-331X/2022/9-ART1 $15.00
https://doi.org/10.1145/nnnnnnn.nnnnnnn

exclusive features often implement the same functionality in different ways, each with a unique performance surface. There are (sometimes unknown) combinations of features that are advantageous or detrimental to performance. Given these hurdles, what product of an SPL achieves the best performance? This is the challenge of SPL *Optimization* (SPLO).

SPLO is daunting. The complexity of feature constraints and the performance influence of features and feature interactions is beyond human reasoning. Simply using default configurations is notoriously bad [7]. To find a configuration with near-optimal performance is known to be difficult [41, 43, 49, 55, 60, 83–85, 88, 91, 94, 100, 103, 115, 127].

The Contestants. There are two known ways to find a *near-optimal configuration* (c_{no}) in a product space: (a) create a *Performance Model* (PM) and use an optimizer ***or*** (b) randomly search using *Uniform Random Sampling* (URS) – every configuration in $\mathbb{C}$ has an equal probability of being selected (*e.g.*, $\frac{1}{|\mathbb{C}|}$ where $|\mathbb{C}|$ is the cardinality of $\mathbb{C}$).

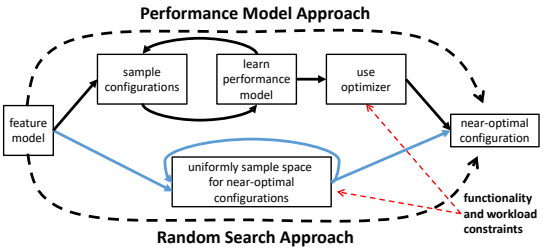

Fig. 1. Performance modeling vs. random searching.

The upper path in Fig. 1 abstracts the process of *Machine Learning* (ML) PMs: a configuration space is randomly (and not necessarily uniformly) sampled; samples are interleaved with model learning until a model is sufficiently accurate. An optimizer uses a PM with a workload and functionality constraints to find a c_{no}.

The bottom path abstracts random searching: a workload-and-functionality-constrained subspace is uniformly sampled until a c_{no} is found.

Why is SPLO hard? Three reasons:

- URS is a gold standard for statistical analysis. Uniformly sampling an enumerated space is easy: randomly select an integer from [1..|$\mathbb{C}$|] and index to that configuration. Enumeration of colossal spaces is infeasible, so non-URS sampling methods are used instead [1, 3, 25, 27, 34, 42, 49, 62, 65]. Probabilistic models of URS are simple, but rarely so for non-URS methods. And each configuration is a solution to a propositional formula; how to index to a solution is unknown.
- Building and benchmarking a configuration is very expensive. Minimizing the sample size to while achieving accuracy is critical to all approaches. Today, only heuristics are known, like: use sample size (f, $2{\cdot}f$, $3{\cdot}f$, ...) where f is the SPL's number of features [42, 46].
- Statistical guarantees on the quality of returned c_{no}s should be required: a c_{no} is within x% of optimal with y% confidence. Such statistical guarantees are unknown today.

1.1 The Central Questions of SPLO

Let a *sample* be a set of configurations, whose cardinality is its *size*. Let c_{best} be a product in $\mathbb{C}$ that has the optimal performance for a given workload and functionality constraints. Then:

(1) How does one find a c_{no} in an SPL configuration space?
(2) How accurate (*e.g.*, how near c_{best}) is the returned c_{no}?
(3) What sample size should be used?

1.2 Contributions of This Paper

- *Order statistics* and URS [10, 126] provide an *SPLO statistical guarantee*: *i.e.*, a returned c_{no} is within x% of optimal with y% confidence;

- Given any two of (a) accuracy (x%), (b) confidence (y%), and (c) sample size, the third can be determined mathematically, which leads to standardized answer tables;
- A scalable algorithm to uniformly sample colossal ($\gg 10^{10}$) configuration spaces;
- Experimental SPLO results comparing c_{no} recommendations of existing ML PMs with those of random search algorithms on enumerable SPLs with $\leq$250K products;
- Experimental SPLO results on random search algorithms in colossal SPL spaces: one has 10^{12} products and another has 10^{81};
- The first solution to the *Fixed Budget* SPLO problem: given a fixed sample size, return the best c_{no} with statistical qualifications using multiple random search algorithms.

2 RESULTS ON PERFORMANCE MODELING

2.1 Basic Facts

Performance Modeling. ML approaches to PM creation are enormously diverse [73, 95]; we do not try to be exhaustive or complete. Instead, we review ideas of *Linear Regression* (L_R), a popular ML approach used in SPLO. Let $\hat{\$}(c)$ be the estimated performance of configuration $c \in \mathbb{C}$. A common form of $\hat{\$}(c)$ is [33, 43, 67, 107, 108]:

$$\hat{\$}(c) = \beta_0 + \beta_1 \cdot x_1(c) + \beta_2 \cdot x_2(c) + \ldots + \beta_h \cdot x_h(c) \quad (1)$$

Consider any $x_i(c)$ term in Eqn (1). Either $x_i(c)$ represents a unique feature, say F_j in Fig. 2a, meaning $x_i(c)$=1 if F_j is present in c; 0 otherwise. *Or* $x_i(c)$ represents a t-way interaction of t>1 distinct features. Suppose $x_i(c)$ is the 3-way interaction of features $\{F_j, F_k, F_q\}$ in Fig. 2b, meaning $x_i(c)$=1 if F_j, F_k, and F_q are all present in c; 0 otherwise. If an SPL has f features, the number of distinct $x_i(c)$ terms is 2^f-1. For any reasonable f, 2^f is far too big. So a typical approach finds 2-way to 5-way interactions that are important to performance [43, 67, 106], so that $h \ll 2^f$ in Eqn (1). Recent research suggests 3-way is sufficient [67].

(a) $x_i(c) = \begin{cases} 1 & \text{if } (F_j \in c) \\ 0 & \text{otherwise} \end{cases}$

(b) $x_i(c) = \begin{cases} 1 & \text{if } (\{F_j, F_k, F_q\} \subset c) \\ 0 & \text{otherwise} \end{cases}$

Fig. 2. Definitions of $x_i(c)$.

Let $\$(c_r)$ be the benchmarked value of configuration c_r. Given a set of $\{(c_r, \$(c_r))\}_{r=1..t}$ pairs, L_R finds the value $B = [\beta_0 \ldots \beta_h]$ that minimizes the sum of the squares of differences between measured and predicted values, *i.e.*, $\min\left\{\sum_{r=1}^{t} \left(\$(c_r) - \hat{\$}(c_r)\right)^2\right\}$ where $B \in \mathbb{R}^{h+1}$ [23].

Optimizer Complexity. All $x_i(c)$ assume the value 0 or 1. Applying the constraints of a feature model so that only legal configurations are examined, optimizing Eqn (1) becomes an instance of 0-1 Linear Programming, which is NP-hard [16, 122]. Although this result is specific to L_R PMs, any comparable formulation will not alter this complexity.

Conclusion: ***An optimizer must solve an NP-hard problem to find*** c_{best}.

Workload and Environment Fragility. A *workload* is a set of tasks that are to be executed by a program. A benchmark measures one or more performance metrics (build size, completion-time, maximum memory footprint, *etc.*) of a program when executing a workload. All ML PM models known to us are created with a fixed workload. It is well-known that changing the workload alters c_{best}; the same for changes in execution environment [6, 7, 15, 29, 128, 130].

Conclusion: ***A PM may need to be relearned if its workload or environment changes.*** More on this in Section 8.2.

2.2 PM Answers to Central Questions

Answers to Section 1.1 questions for contemporary PM research are:

(1) A PM "fits" a line or curve through a set of observations $\{ (c_r, \$(c_r)) \}_{r=1..t}$. Prediction errors are unavoidable, although errors are minimized.
(2) Unless an SPL configuration space is enumerated and benchmarked, it is unknown how close a c_{no} is to c_{best}. Of course, enumeration is impractical or impossible in most circumstances.
(3) The sample size to use depends on the learning algorithm (see SPLConqueror in Section 5.1), although there are rules-of-thumb: let f be the number of SPL features. Start with a sample size f, build a model, and compute its accuracy α. If α is too low, repeat the process until a budget of configurations or an acceptable accuracy is reached, *i.e.*, (f, $2{\cdot}f$, $3{\cdot}f$, ...) [42, 46].

3 RESULTS ON SIMPLE RANDOM SEARCHING

3.1 Performance Configuration Space (PCS) Graphs

Imagine it is possible to benchmark every $c \in \mathbb{C}$, where $\$(c)$ is c's measured performance. Small $ is good (efficient) and large $ is bad (inefficient). Sort all $(c, \$(c))$ pairs in increasing $\$(c)$ order and plot them equally-spaced along the X-axis. The result is a *Performance Configuration Space* (PCS) graph. A *normalized* PCS graph normalizes the X-axis to the unit interval [0..1], where c_{best}=0 and c_{worst}=1. The Y-axis is similarly normalized, where $\$(c_{best})$=0 and $\$(c_{worst})$=1. See Fig. 3 [91].

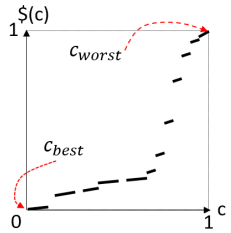

Fig. 3. A PCS graph.

All SPLs have finite (perhaps colossal) configuration spaces. Consequently, their PCS graphs are discrete, discontinuous and stair-stepped like Fig. 3, because consecutive configurations along the X-axis encode discrete decisions/features that make discontinuous jumps in performance [78]. Further, every PCS graph is monotonically non-decreasing; consecutive configurations along the X axis, like c_i and c_{i+1}, satisfy $\$(c_i) \leq \$(c_{i+1})$, as some features have no impact on performance.

Random search algorithms are well-suited for non-differentiable and discontinuous functions, like PCS graphs.

3.2 Simple Random Search (SRS)

URS requires every configuration to have equal probability $\frac{1}{|\mathbb{C}|}$ to be selected. Given that $|\mathbb{C}|$ is colossal, we can approximate a discrete distribution with the continuous distribution Uniform(0,1):

$$\lim_{|\mathbb{C}|\to\infty} \frac{1}{|\mathbb{C}|} \cdot \left[\, 1 \,..\, |\mathbb{C}| \,\right] = \lim_{|\mathbb{C}|\to\infty} \left[\, \frac{1}{|\mathbb{C}|} \,..\, \frac{|\mathbb{C}|}{|\mathbb{C}|} \,\right] = [0..1] \tag{2}$$

The *Simple Random Search* (SRS) algorithm uniformly selects n configurations from $\mathbb{C}$, *i.e.*, n points from [0..1]. *On average,* n points partition [0..1] into n+1 equal-length segments. The k^{th}-best configuration out of n, denoted $c_{k,n}$, has expected rank $\frac{k}{n+1}$. The $k{\cdot}\binom{n}{k}$ term in Eqn (3) is a normalization constant [10, 126]:

$$c_{k,n} \;=\; k \cdot \binom{n}{k} \cdot \int_0^1 x^{k-1} \cdot (1-x)^{n-k} \cdot dx \;=\; \frac{k}{n+1} \tag{3}$$

The expected *rank* or distance c_{no} is from c_{best} is:

$$c_{1,n} \;=\; \frac{1}{n+1} \tag{4}$$

Let's pause to appreciate this result. The lone axis of Fig. 4 represents the X-axis of all PCS graphs. As the sample size n increases, c_{no} progressively moves closer to c_{best} at X=0, Fig. 4a→4c. *If a sample size of 99 is used,* c_{no} *will be 1%, on average, from* c_{best} *in ranking along the X-axis.*

Note: Eqns (3)-(4) do not reference $|\mathbb{C}|$; $|\mathbb{C}|$ disappeared when the limit was taken in (2). This means Eqns (3)-(4) predict c_{no} X-axis ranks for an *infinite-sized configuration space*. Only for tiny spaces, $|\mathbb{C}| \leq 1000$, will predictions by Eqns (3)-(4) be low. See Appendix A.

How accurate is the $\frac{1}{n+1}$ estimate? Answer: We can compute $v_{1,n}$, the second moment of $c_{1,n}$, and then the standard deviation $\sigma_{1,n}$ of $c_{1,n}$ [16, 81]:[2]

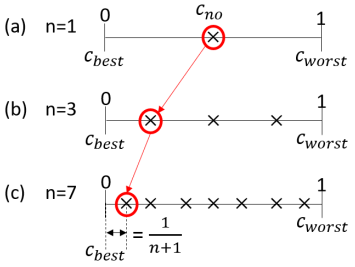

Fig. 4. URS in action.

$$v_{1,n} = 1 \cdot \binom{n}{1} \cdot \int_{\emptyset}^{1} x^2 \cdot (1-x)^{n-1} \cdot dx = \frac{2}{(n+1)\cdot(n+2)} \tag{5}$$

$$\sigma_{1,n} = \sqrt{v_{1,n} - {c_{1,n}}^2} = \sqrt{\frac{2}{(n+1)\cdot(n+2)} - \left(\frac{1}{n+1}\right)^2} \tag{6}$$

For large n, Eqn (6) converges to $\sqrt{\frac{2}{n^2} - \frac{1}{n^2}} = \frac{1}{n}$, which equals $c_{1,n} = \frac{1}{n}$. Fig. 5 shows the convergence rate:

$$\%\mathtt{diff} = 100 \cdot \left(\frac{c_{1,n}}{\sigma_{1,n}} - 1\right) \tag{7}$$

When n=50, $c_{1,n}$ is 2% larger than $\sigma_{1,n}$. For n≥200, there is no practical difference between theoretical $c_{1,n}$ and $\sigma_{1,n}$ values, *i.e.*, the standard deviation of $c_{1,n}$ is small.

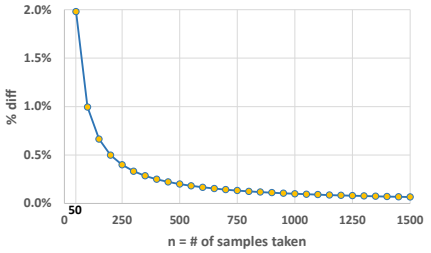

Fig. 5. Difference of $\sigma_{1,n}$ and $c_{1,n}$.

Readers may have noticed that our configuration ranking is along the X-axis, not the Y-axis. This is a *percentile*. In SPLO, the goal is to be in the smallest percentile: ≤1% means "in the top 1 percentile".

Conclusion: ***To find a c_{no} in a colossal product space, SRS takes a uniform sample of size n, builds and benchmarks each configuration, and returns the best performing configuration, c_{no}, that on average is the top $\frac{100}{n+1}$ percentile of all products with a standard deviation of $\frac{100}{n+1}$ percentile.***

3.3 How to uniformly sample an SPL configuration space

Every SPL has a feature model F that can be translated into a propositional formula ϕ [9, 13, 14]. A #SAT tool can count the number of solutions to ϕ efficiently [111]. We know $|\phi| = |\mathbb{C}|$. Let cfc be the client functionality constraints on ϕ. The predicate for a user-constrained space is $\phi \wedge \mathtt{cfc}$.

Alg. 1[3] samples a configuration by assigning a Boolean value to each feature $f_1, f_2, \ldots, f_\omega$ in F. First, f_1 is randomly assigned according to its probability $p_1 = \frac{|\phi \wedge f_1|}{|\phi|}$ of being true in any configuration. Suppose f_1 is assigned to false. Then, f_2 is randomly assigned according to its probability p_2 of being true in a configuration conditioned to f_1's prior assignment: $p_2 = \frac{|\phi \wedge \neg f_1 \wedge f_2|}{|\phi \wedge \neg f_1|}$.

This procedure advances until the last feature f_ω is assigned, thereby completing a uniformly random configuration. A formal proof of Alg. 1's uniformity is given in Appendix B.

[2] The integrals of this section were evaluated by Mathematica 12.1.1.0.

[3] Knuth first sketched this algorithm in 2009 [66]. Batory reinvented it in 2016 unaware of his work. Oh was first to implement it with practical improvements: using Heule's cube-and-conquer algorithm to find an efficient ordering of features to partition the space [52], caching #SAT computations to avoid repeated evaluations, replacing the remaining last g bits to assign when they are "don't cares" with a random g-bit number, and (optionally) caching configurations to remove duplicates thereby achieving sampling-without-replacement [91].

Algorithm 1: Uniform Random Sampling (URS)

Configuration URS(ϕ, $\mathbb{F}$):
  Input : ϕ feature model propositional formula $\wedge$ client functionality constraints
  $\mathbb{F}$ = $(f_1, f_2, \ldots, f_\omega)$ be a static list of all features in the feature model, to which no Boolean value has been assigned
  Output : a random configuration composed of Boolean assignments a_i for each $f_i \in \mathbb{F}$

$|\phi| \leftarrow$ #SAT computes the number of solutions to ϕ;
for *each* i *in* $(1..\omega)$ **do**
  $|\phi \wedge f_i| \leftarrow$ #SAT computes the number of solutions to $\phi \wedge f_i$;
  Generate an independent random value j uniformly distributed in [0,1];
  if $j \leq \frac{|\phi \wedge f_i|}{|\phi|}$ **then**
    $a_i \leftarrow$ true; $\phi \leftarrow \phi \wedge f_i$; $|\phi| \leftarrow |\phi \wedge f_i|$;
  else
    $a_i \leftarrow$ false; $\phi \leftarrow \phi \wedge \neg f_i$;
    $|\phi| \leftarrow$ #SAT computes the number of solutions to $\phi \wedge \neg f_i$;
return $(a_1, a_2, \ldots . a_\omega)$;

BDDSampler. A new tool, called BDDSampler [17, 50], implements an optimized version of Alg. 1 [91]. BDDSampler is built on top of the CUDD [31] library for BDDs and is remarkably fast, even for colossal spaces. The last column in Table 2 shows the time BDDSampler needed to sample 1,000 configurations with replacement for different SPLs[4] averaged over 100 executions.[5] The 3rd column in Table 2 lists the BDD synthesis times for feature models by the procedure of [35].[6]

SRS requires (i) building a BDD structure, (ii) sampling configurations, (iii) building products, and (iv) benchmarking products. Actions (i)-(ii) can be done relatively quickly, but (iii)-(iv) are computationally expensive, and that is why minimizing the sample size is critical to both SPLO and ML performance [79]. For example, sampling all 26,256 configurations of JHipster with BDDSampler took 4.48 seconds.[5,7] However, building and benchmarking all 26,256 configurations took 4,376 hours of CPU time (182 days approximately or 10min/build-and-benchmark) and needed 5.2 terabytes of disk on the INRIA supercomputer Grid'5000 [48].

SPL	$\lvert\mathbb{C}\rvert$	Time (secs)	
		Synthesis	Sampling
JHipster 3.1.6	$2.6{\cdot}10^4$	0.01	0.04
DellSPLOT	$7.4{\cdot}10^6$	0.29	0.08
Fiasco 2014092821	$5.1{\cdot}10^9$	0.14	0.07
axTLS 1.5.3	$3.9{\cdot}10^{12}$	0.05	0.04
ToyBox 0.5.2	$1.5{\cdot}10^{17}$	0.02	0.25
uClibc 201 50420	$7.5{\cdot}10^{50}$	0.41	0.14
BusyBox 1.23.2	$7.4{\cdot}10^{146}$	0.62	0.26
EmbToolkit 1.7.0	$4.0{\cdot}10^{334}$	4304.68	2.61
LargeAutomotive	$5.3{\cdot}10^{1441}$	21.50	12.07

Table 2. BDDSampler sampling time for 1,000 configurations.

3.4 What Sample Size to Use?

A basic question for any SPLO sampling method is: What sample size is needed to find a near-optimal solution for a given accuracy? As rigorous analyses are usually not cited by the authors of proposed non-URS methods (*e.g.,* [30, 34, 40, 42, 49, 82]), this question may have no answer. URS does. Let

[4] The BDDs of the SPLs in Table 2 are available at: https://doi.org/10.5281/zenodo.4514919
[5] An Intel(R) Core(TM) i7-6700HQ, 2.60GHz, 16GB RAM, operating Linux Ubuntu 19.10 was used.
[6] The tool used to synthesize the BDDs is available at: https://github.com/davidfa71/Extending-Logic
[7] We did not *enumerate* all configurations but *sampled* them by running: BDDSampler -norep 26256 JHipster.dddmp, which asks BDDSampler to generate 26,256 random configurations *without replacement* from a BDD that encodes the JHipster feature model.

ρ be the desired percentile of accuracy (*e.g.*, top 1% sets ρ=.01). Each selected configuration is a Bernoulli trial. The confidence/probability ¢ that a uniform sample of size n returns a c_{no} in the top ρ accuracy is Eqn (8):

$$¢ = 1 - (1 - \rho)^n \tag{8}$$

Solving for n yields Eqn (9):

$$n = \frac{\ln(1 - ¢)}{\ln(1 - \rho)} \tag{9}$$

Table 3 lists the sample size that achieves a given confidence (¢) and accuracy (ρ) *for an infinite-sized space*. Example: A configuration in the top 2% of $\mathbb{C}$ with 95% confidence is returned when n=148.

Other tables can be derived from Eqn (8) for accuracy (ρ) and confidence (¢). Table 4(a) says a budget of 100 samples and 95% confidence returns a configuration in the top 2.95% of all solutions.

n = sample size	¢ = %confidence			
ρ = %accuracy	90.0%	95.0%	98.0%	99.7%
5.00%	45	58	76	113
4.00%	56	73	96	142
3.00%	76	98	128	191
2.00%	114	148	194	288
1.00%	229	298	389	578
0.50%	459	598	780	1159
0.30%	766	997	1302	1933
0.20%	1150	1496	1954	2902
0.10%	2301	2994	3910	5806

Table 3. Sample Size n given ¢ and ρ.

ρ = %accuracy	n = sample size						
¢ = %confidence	25	50	100	200	400	800	1600
90.0%	8.80%	4.50%	2.28%	1.14%	0.57%	0.29%	0.14%
95.0%	11.29%	5.82%	2.95%	1.49%	0.75%	0.37%	0.19%
98.0%	14.49%	7.53%	3.84%	1.94%	0.97%	0.49%	0.24%
99.7%	20.73%	10.97%	5.64%	2.86%	1.44%	0.72%	0.36%

(a)

¢ = %confidence	n = sample size						
ρ =% accuracy	25	50	100	200	400	800	1600
4.000%	64.0%	87.0%	98.3%	100.0%	100.0%	100.0%	100.0%
2.000%	39.6%	63.6%	86.7%	98.2%	100.0%	100.0%	100.0%
1.000%	22.2%	39.5%	63.4%	86.6%	98.2%	100.0%	100.0%
0.500%	11.8%	22.2%	39.4%	63.3%	86.5%	98.2%	100.0%
0.250%	6.1%	11.8%	22.1%	39.4%	63.3%	86.5%	98.2%
0.125%	3.1%	6.1%	11.8%	22.1%	39.4%	63.2%	86.5%

(b)

Table 4. Tables for Expected Accuracy and Confidence

3.5 Why URS is Important

What is the value μ of configuration space property λ? Answer: take a uniform sample of size n and benchmark each configuration to obtain its λ value. Then compute the mean $\overline{\mu}$ and standard deviation s of sampled λ values. By the *Central Limit Theorem* (CLT) [114], the true population mean μ is contained in the following confidence interval:

t	n=sample size						
¢=%confidence	25	50	100	200	400	800	1600
90.0%	1.71	1.68	1.66	1.65	1.65	1.65	1.65
95.0%	2.06	2.01	1.98	1.97	1.97	1.96	1.96
98.0%	2.49	2.4	2.36	2.35	2.34	2.33	2.33
99.7%	3.3	3.12	3.04	3	2.99	2.98	2.97

Table 5. t-values given ¢ and n.

$$\left(\overline{\mu} - t \cdot \frac{s}{\sqrt{n}}\right) \le \mu \le \left(\overline{\mu} + t \cdot \frac{s}{\sqrt{n}}\right) \tag{10}$$

where t is determined from Student's t-distribution given a desired confidence level ¢ and sample size n. Table 5 lists t values for some combinations of ¢ and n [114]. **Note:** *A precondition of* CLT *and Eqn (10) is that samples are uniform.*

Example. Let μ be the average number of features that are present in a configuration. Fig. 6 plots μ estimates for two SPLs with different sampling methods and sample sizes. The X-axis is n, the sample size, and the Y-axis is μ estimates. The straight line (—) indicates the correct μ as these SPLs are small enough to enumerate and compute the correct answer. The dashed lines indicate the 95% confidence envelope for each μ estimate, Eqn (10). ✖ marks estimates by URS. Sampling

methods ▲ and ◇ are proposed as alternative methods to URS: ▲ is QuickSampler [34] and ◇ is DDbS [62]. [8] Observe:

- All three μ estimates converge to an answer with increasing n;
- URS correctly estimates μ with increasing accuracy; other methods converge to different incorrect answers;
- Method ◇ selects different sample sets each time in Fig. 6b, but oddly the same number of features occurs in all samples. Thus, the estimate by ◇ is suspicious as it lacks variability.

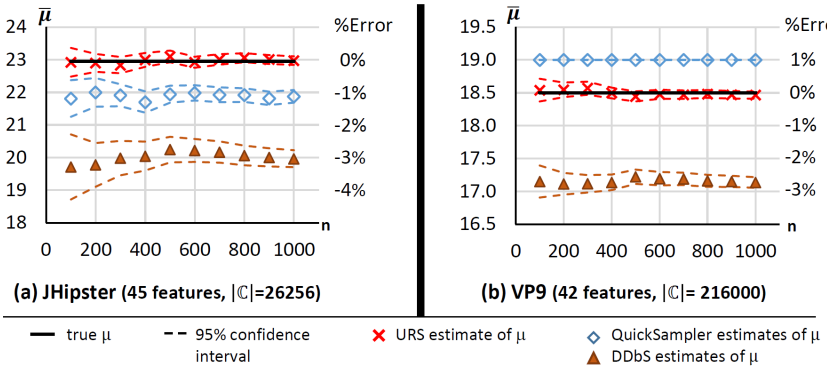

Fig. 6. Why URS is Important.

Conclusion: ***Classical statistical methods assume URS as a precondition; if this precondition is violated, computed statistics are suspect [21].*** Other benefits of URS include:

- Population statistics (like μ) can be predicted by probability analyses. URS can confirm the correctness of these predictions; and
- When analytical predictions are unavailable, URS can estimate population statistics that a correct analysis would return.

3.6 PCS Graphs of Enumerable and Non-Enumerable SPLs

What do real PCS graphs look like? This is not a fundamental question, but one asked of curiosity. Several small SPLs were enumerated and benchmarked by Siegmund *et al.* [105, 106], which took months to complete. From his data, we computed their unnormalized PCS graphs, Fig. 7.

- **Apache** is an open-source Web server [8]. With 9 features and 192 configurations, the maximum server load size was measured through `autobench` and `httperf`;
- **LLVM** is a compiler infrastructure in C++ [75]. With 11 features and 1024 configurations, test suite compilation times were measured;
- **H264** is a video encoder library for H.264/MPEG-4 AVC format written in C [45]. With 16 features and 1152 configurations, Sintel trailer encoding times were measured; and
- **BerkeleyDBC** is an embedded database system written in C [19]. With 18 features and 2560 configurations, benchmark response times were measured.

A *complete PCS graph* plots every point in $\mathbb{C}$; this is possible when an SPL configuration space is enumerable. But what about spaces that are too large to enumerate? A number of techniques were tried, and the simplest worked best:

[8] From prior experiments [92], we knew that samples from these methods were *not* uniform and Eqn (10) was not applicable. We wondered how they performed *w.r.t.* URS as they were proposed as URS substitutes.

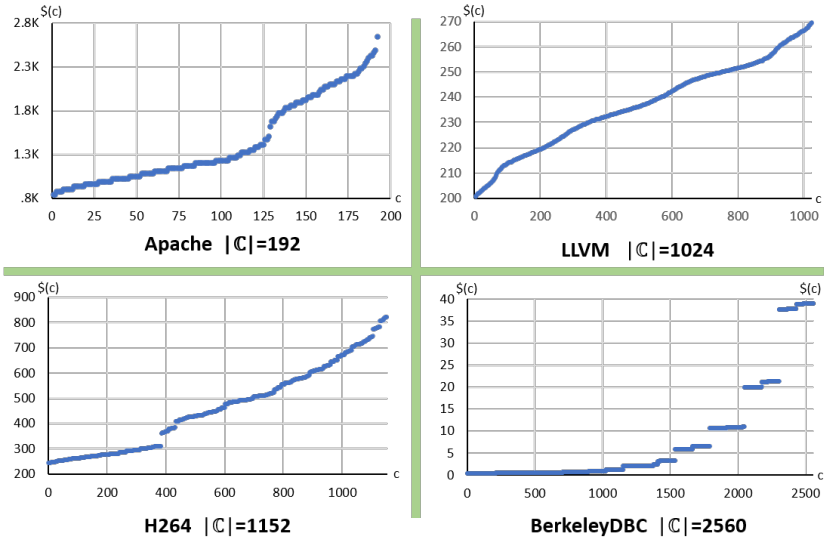

Fig. 7. Complete PCS graphs for enumerable SPLs – raw data by Siegmund [105, 106].

(1) Take a uniform sample of size n=100 or n=200 as this (to us) yields a *minimal fidelity* PCS graph;
(2) For each configuration c, build and benchmark it to measure $(c);
(3) Sort the (c, $(c)) tuples from best-performing to worst;
(4) Let y_i be the i^{th} best performance. Plot a PCS graph using these points $\left\{\left(\frac{i}{n+1}, y_i\right)\right\}_{i=1}^{n}$.

Example. uClibc-ng is a C library for embedded Linux systems with 269 features and $|\mathbb{C}|=\sim 8\times 10^{26}$ [90]. A minimum fidelity (n=200) PCS graph of uClibc-ng is Fig. 8. Build size was measured.

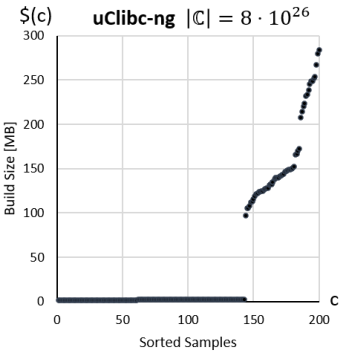

Fig. 8. uClibc-ng PCS graph.

3.7 SRS Answers to Central Questions

Section 1.1 listed three questions; SRS offers elegant answers for each:

(1) How does one find a c_{no} in an SPL configuration space? **Answer:** Take a uniform sample of size n, benchmark each configuration, and return the best-performing configuration, c_{no};
(2) How accurate (*e.g.*, how near c_{best}) is the returned c_{no}? **Answer:** On average, the c_{no} is $\frac{100}{n+1}$ percentiles from c_{best} with standard deviation of $\frac{100}{n+1}$ percentiles; and
(3) What sample size should be used? **Answer:** Choose a desired accuracy and confidence for a c_{no}, and use Table 3 to determine the sample size.

4 RECURSIVE RANDOM SEARCH (RRS)

We believe SRS offers a minimal performance bound for every SPLO algorithm, as more sophisticated algorithms and those that exploit domain-specific knowledge should perform better. In this section, we review another promising random search algorithm. There are no replacements for SRS yet; a replacement would have an SPLO statistical guarantee on the c_{no}s it returns.

RRS. A c_{no} will be in the top $\frac{1}{1+9}$=10% percentile using a uniform sample of size 9. Increasing the solution precision to the top $\frac{1}{1+99}$=1% requires a sample size of 99, 11× larger. Suppose from the first 9 configurations feature F is inferred to be common to configurations in the top 10%. If the scope of the search is restricted to $(\phi \wedge F)$ and another uniform sample of size 9 is taken, a near-optimal solution would be within $\frac{1}{1+9} \cdot \frac{1}{1+9} = \frac{1}{100}$=1%, for a total of 18 configurations; a 5.5× improvement. This is *Recursive Random Search* (RRS).

Implementation. A rule-of-thumb for c_{best} is that it contains some of the top performance-enhancing features of an SPL [22]. We call such features *noteworthy*. The twist is that some features become noteworthy only in the presence of other noteworthy features.

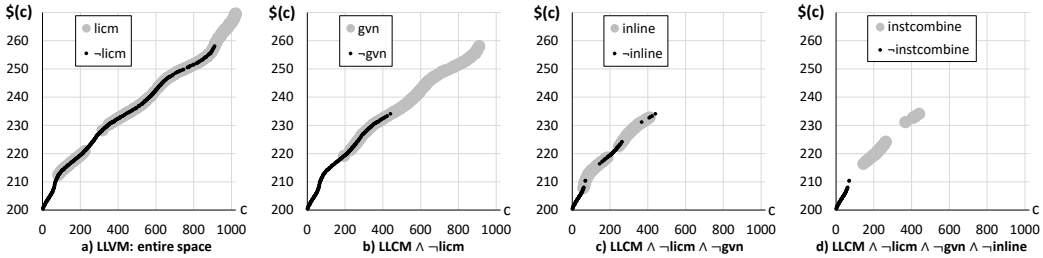

Fig. 9. Stairs of LLVM.

Consider the PCS graph of LLVM, Fig. 9a. This graph is almost linear. Look how noteworthy features (f or ¬f) present themselves in Fig. 9a-d, in order of most-influential to next-most-influential, and so on, recursively restricting the next subspace to search.

We mechanized the noteworthy procedure by: (1) qualifying features to consider, as not all are relevant, (2) checking selected features for compability, (3) filtering remaining features based on their performance influence.

First, we found experimentally that examining only the features of the top configuration T_1 was misleading – some noteworthy features of T_1 do not belong to c_{best} and by selecting them assures RRS never reaches c_{best}. Examining features shared by the top two configurations (T_1, T_2) was less misleading. And shared features in the top three ($T_1..T_3$) configurations was too constraining, as important features may not be in all three configurations.

Second, let S be the features common to T_1 and T_2. A SAT solver was not needed to validate that features of S are compatible (meaning no feature(s) of S precludes another). All features of T_1 are compatible, and so too is any subset. Any shared subset among T_1 and T_2 must also be compatible.

Third, let N configurations be uniformly sampled per recursion.[9] For every sampled configuration c, we know its features and its measured performance $(c). Now, what features of S are noteworthy? **Answer**: Consider each feature f∈S. Compute the average performance $\bar{\$}(f)$ of configurations sampled sofar ***with*** feature f, and the average performance $\bar{\$}(\neg f)$ of configurations ***without*** f. Their difference $\$\Delta(f)$ is the *performance influence* of f:

$$\$\Delta(f) \;=\; \bar{\$}(f) - \bar{\$}(\neg f) \tag{11}$$

[9] See Section 6 for additional constraints on RRS termination, which samples ≤ N configurations on the last recursion.

Algorithm 2: Recursive Random Search (RRS)

```
1  Configuration RRS(N, φ, NW):
       Input  : N    number of configurations per recursion
                φ    feature model propositional formula ∧ client functionality constraints
                NW   set of noteworthy features (set to empty on initial call)
       Output:       best configuration found
2      sample ← randomly sample N configurations from φ ∧ NW;
3      sort sample so that sample[0] has best performance, and sample[1] has next best;
4      commons ← negative or positive features common to sample[0] and sample[1];
5      for each f in commons do
6          if (Δ(f) < 0) ∧ MannWhitneyUTest(f) then
7              add f to NW;
8      if (NW unchanged from previous recursion) or (N ≥ |φ∧ previous NW|) then
9          return sample[0] ; // best configuration found
10     else
11         return RRS (N, φ, NW);
```

The sign of $\$\Delta(f)$ indicates whether f ***improves*** (negative value) or ***degrades*** (positive value) average performance. Further, a `t-test` [38] checks whether $\$\Delta(f)$ is statistically significant with 95% confidence; if significant, f is noteworthy else it is discarded.[10] RRS is Alg. 2.[9]

Comparison. The accuracy of SRS and RRS can be compared by experiments that compute the true average rank $\bar{\mu}$ of solutions (which is possible for enumerable SPLs) to the theoretical accuracy of SRS for a sample size n, $\frac{1}{n+1}$ *a.k.a.* Eqn (4). The experiment uses:

- N as the number of configurations per RRS recursion; and
- n as the total number of configurations taken by RRS.

Fig. 10 plots averages of 100 experiments for different SPLs and different N. While both $\bar{\mu}$ and $\frac{1}{n+1}$ decrease sharply with increasing N, $\bar{\mu}$ is on average better than $\frac{1}{n+1}$.

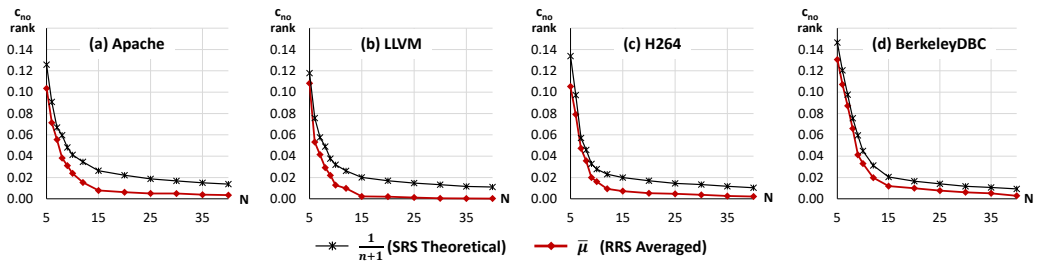

Fig. 10. Comparison of SRS and RRS.

Key limitations of RRS are:

- It is ***not*** always better than SRS when the N (configurations per recursion) is too small; and
- It lacks analyses like c_{no} rank prediction (Eqn (4)) and confidence guarantees (Eqn (8)).

A solution to these limitations is given in Section 7. The next sections evaluate SRS and RRS.

[10] A typical rule-of-thumb [38] states that the Central Limit Theorem holds whenever the sample size is ≥ 30. Accordingly, the distribution of the *sample means* is normal and thus the performance contribution of each feature is estimated by subtracting means and using a `t-test`. However, when $N<30$, a more robust estimator and a non-parametric test is required; in particular, the feature's performance is calculated by $\Delta(f)$=median$(\$(f))$−median$(\$(\neg f))$, and statistical significance checked with a `Mann-Whitney U-test` [77]

5 EVALUATION USING ENUMERABLE SPLS

SPL researchers used enumerable SPLs ($|\mathbb{C}| \leq 250K$) as benchmarks with metrics for overall accuracy (MAPE, defined in Section 5.4) and, to a lesser extent, solution accuracy (average rank of returned c_{no}s) and reliability (standard deviation of returned c_{no}s) to compare different PM algorithms [42, 46, 47, 62, 88]. We adopt these guidelines.

Using the same sample size or smaller, an SPLO algorithm is *more accurate* than others if it finds better solutions (c_{no}s) and is *more reliable* than others if its solutions have a smaller standard deviation (σ). A higher σ means solutions vary more.

We ask the following research questions about SPLO algorithms:

- **RQ1**: Which algorithm is the most accurate across selected SPLs?
- **RQ2**: Which algorithm is the most reliable across selected SPLs?
- **RQ3**: Are PM accuracy and PM solution accuracy correlated?

5.1 Evaluation Setup

Enumerated spaces allow us to (a) know the true PCS rank of a c_{no} and (b) compute the difference of a c_{no}'s true performance $\$(c_{no})$ from a PM's estimate $\hat{\$}(c_{no})$. Taken from [105, 106], the SPLs are:

- BerkeleyDBC is an embedded database system with 18 features and 2,560 configurations [19]. Benchmark response times were measured;
- 7z is a file archiver with 44 features and 68,640 configurations [2]. Compression times were measured; and
- VP9 is a video encoder with 42 features and 216,000 configurations [116]. Video encoding times were measured. To our knowledge, VP9 is the largest SPL that has been enumerated.

Each successive SPL in the above list has a configuration space that is ~10× larger than its predecessor. Fig. 11 shows their unnormalized PCS graphs.

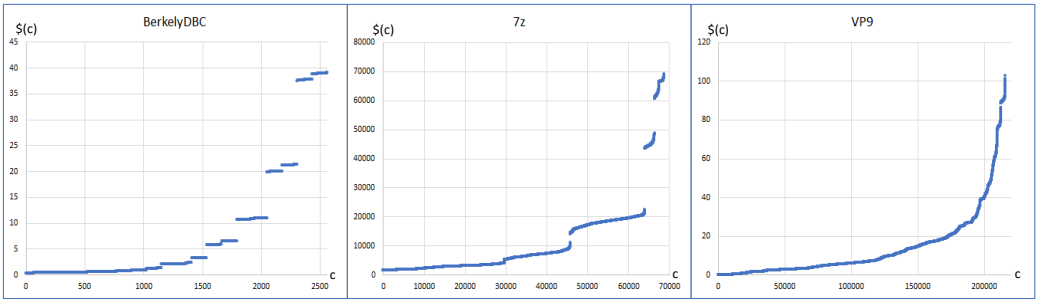

Fig. 11. PCS graphs of selected enumerable SPLs.

We compare SRS and RRS with two PMs: SPLConqueror [107] and DeepPerf [46]. DeepPerf is a state-of-the-art deep sparse neural network that outperformed other major PMs in 2019, including CART [43], DECART [42], Fourier [93], and SPLConqueror. We include SPLConqueror as it is the state-of-the-art in L_R PMs, using linear regression as described in Section 2.

Recall the purpose of a PM is to predict the performance of any configuration in $\mathbb{C}$. It is *not* to find an optimal or near-optimal solution. That is the purpose of an optimizer. We explained in Section 2.1 that finding c_{best} by an optimizer is NP-hard. To discount this difficulty, we use a *perfect optimizer* that returns the optimal configuration according to its PM *for free* by using the PM to evaluate $\min_{c \in |\mathbb{C}|} \hat{\$}(c)$. Of course, such an optimizer is impractical but can be emulated for enumerable configuration spaces. So the conclusions of this section favor PMs.

For SRS and DeepPerf, we ran experiments with sample sizes 50, 100, 200, 500, and 1000. DeepPerf asks for the sample size to use and the number of experiments; hyperparameters for its neural network are configured automatically. For RRS, we ran experiments with N∈{15, 20, 30, 50, 100, 200} configurations per recursion and summed the total number of configurations used after RRS terminates. Remember RRS does not perform well *w.r.t.* SRS when too few configurations per recursion are used. RRS has a *minimum sample size* (MinSS) whose value is revealed by experiments **RQ1** and **RQ2**.

For SPLConqueror, the settings of Kaltenecker *et al.* were used [62]. All five sampling methods of SPLConqueror were evaluated, each producing a distinct PM. Diversified Distance-Based Learning, which we label as S2, was reported to have the best prediction accuracy.[11] For each sampling method, three different sample sizes were used, corresponding to t-way population sizes t ∈ {1, 2, 3}, although some SPLConqueror algorithms used additional configurations whose numbers we could not control but did report. See [62, 107] for more details.

Each experiment was repeated 100 times averages are reported. 100 was chosen so that our evaluations would finish in two weeks of compute time. Statistical significance tests are reported in Appendix C for those interested. Our source code and experimental data are available at https://doi.org/10.5281/zenodo.7485062.

5.2 RQ1: Which algorithm is the most accurate across selected SPLs?

Let n be the number of configurations benchmarked by a PM in an experiment; $\overline{n}$ the average over 100 experiments. Let μ_x be the percentile rank of its c_{no}s, also averaged over 100 experiments. μ_x=5% means that the c_{no}s returned by a PM are in the top 5% (.05 percentile), on average, from c_{best}.

The lines of Fig. 12 (next page) connect $(\overline{n}, \mu_x)$ points of each PM. SPLConqueror has 5 lines, one for each sampling method. Fig. 12a-c show the full results; Fig. 12d-f show a top 5% (.05 percentile) magnified view. Tables (not graphics) for Fig. 12 are in our Zenodo download.

We found:

- SRS and RRS exhibited the overall best performance;
- When using ≤20 configs/recursion, SRS dominates RRS in all but one point in 7z, Fig. 12e. When ≥30 is used, RRS dominates SRS for all SPLs. This discussion continues in **RQ2**;
- When RRS uses >200 configurations total, it returns a c_{no} whose normalized rank is less than 0.2% on average, compared to the theoretical SRS c_{no} normalized rank of 0.5%, Eqn (4);
- The μ_x of SPLConqueror PMs varied, depending on the sampling method and sample size. S2 dominated other SPLConqueror algorithms and outperformed RRS in BerkeleyDBC and 7z. No SPLConqueror algorithm outperformed SRS or RRS in VP9 (the largest SPL space);
- DeepPerf under-performed SRS and RRS for all sample sizes and SPLs. DeepPerf dominated SPLConqueror on VP9, but under-performed BerkeleyDBC and 7z except on three points.

With respect to better c_{no} accuracy with larger sample sizes, we observed:

- SRS and RRS steadily improved μ_x values with increasing sample sizes in all SPLs. SRS and RRS produced the most consistent results;
- More configurations did ***not*** assure better c_{no}s for PMs. DeepPerf found progressively better c_{no}s as sample sizes increased to 500 but did not consistently improve c_{no}s afterward;
- SPLConqueror PM c_{no}s varied considerably. Only two results, S2 and S3 in VP9, showed strictly improving c_{no}s with increasing sample size.

[11] S1 is Distanced-Based, S2 is Diversified Distance-Based, S3 is Solver-Based, S4 is uniform sampling from an enumerated configuration space, and S5 is Randomized Solver-Based [62].

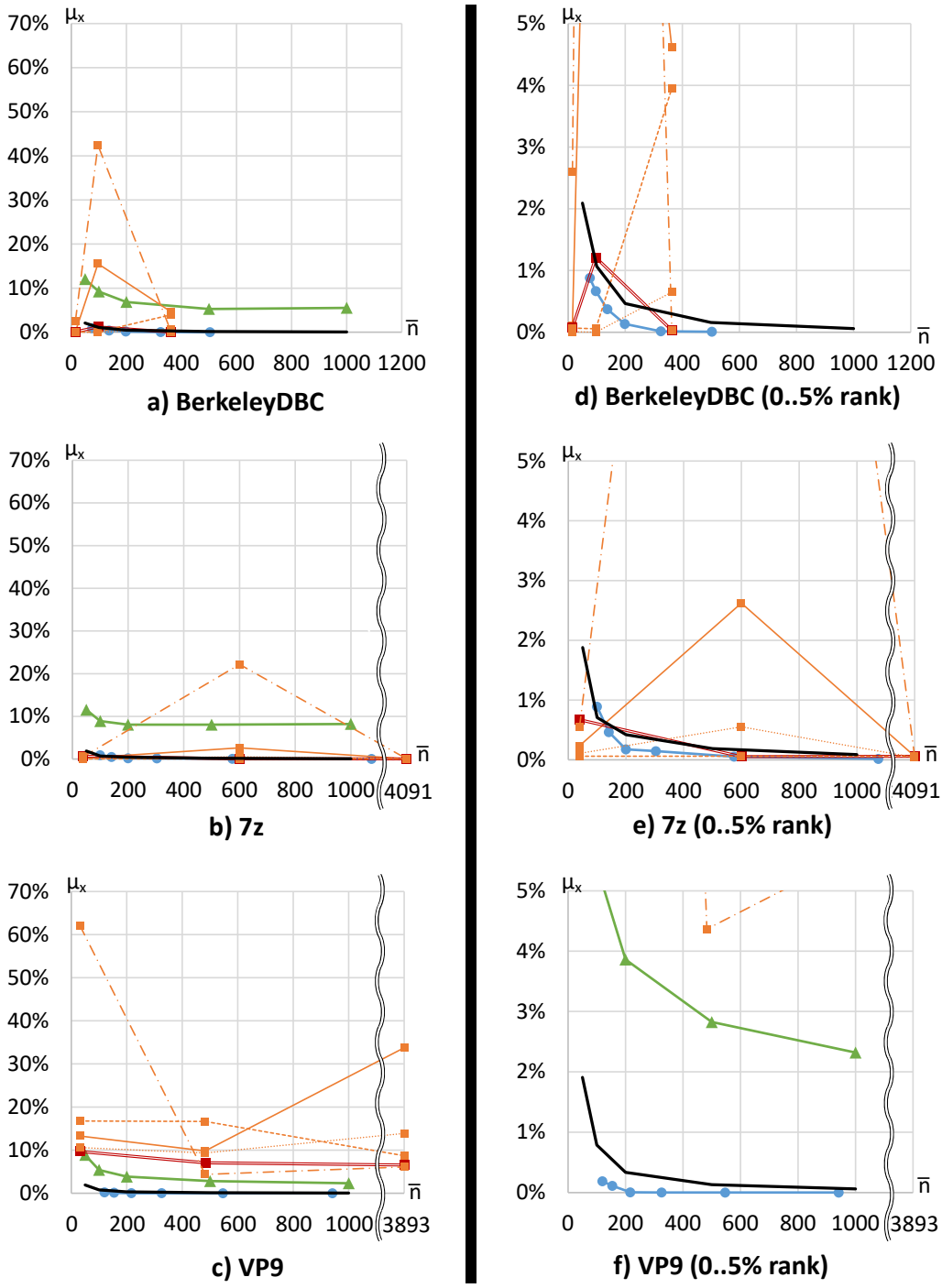

Fig. 12. Average percentile rank (μ_x) *vs.* Average Sample Size ($\bar{n}$) by SPL and SPL0.

With respect to theoretical predictions:

- Fig. 13(a) shows the μ_x of SRS with sample size n matches Eqns (4)-(6). The μ_x of 7z and VP9 measurements are slightly lower than theoretical μ_x as some configurations exhibit the same performance but the rank that we assigned measured the number of configurations that have *better* performance. This possibility is evident in the flat shelf of configurations approaching the origin in the PCS graphs of these SPLs (Fig. 11).

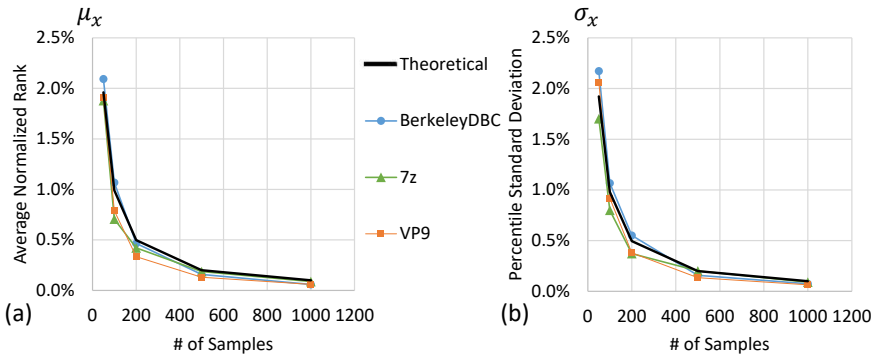

Fig. 13. SRS Theoretical (μ_x, σ_x) and Experimental (μ_x, σ_x).

Summarizing Fig. 12:

- RRS generally outperforms SRS, DeepPerf and SPLConqueror over a wide range of different sample sizes in different SPLs.
- SRS and RRS c_{no}s progressively move toward the origin (c_{best}) of each PCS graph as sample sizes increase. DeepPerf c_{no}s plateau for BerkeleyDBC and 7z.
- We consider SRS as a "minimal performance bound" for SPLOs, as it relies only on URS. DeepPerf failed to outperform SRS for all plotted 45 points in Fig. 12. SPLConqueror failed to outperform SRS in 28-of-45=62% plotted points.[12] These results raise a general concern on the c_{no} accuracy of PMs.
- SPLConqueror outperformed RRS in 12-of-45=27% of the data points in Fig. 12.[13] However, the sampling method and sample size that yielded these results were unknown before these experiments. A priori, it is not obvious which SPLConqueror algorithm to use ahead of time.
- A perfect optimizer was used, which biases the results of this section toward PMs.

Conclusion: ***Sampling (esp. RRS) produced the best μ_x solutions in these experiments.***

5.3 RQ2: Which algorithm is the most reliable across selected SPLs?

The standard deviation σ_x of μ_x measures the reliability of solutions returned by SPLO algorithms. The larger the σ_x, the less stable or more variable the result; the smaller the σ_x, the better.

The lines of Fig. 14 (next page) connect $(\bar{n}, \sigma_x)$ points of each SPLO algorithm. Fig. 14a-c are the full results; Fig. 14d-f show a magnified top 5% (.05 percentile) view. Tables (not graphics) for Fig. 14 are in our Zenodo download. We found:

[12] SRS bettered SPLConqueror on 6 points of BerkeleyDBC, 7 in 7z, and 15 in VP9, for a total of 28-of-45=62%. Some SPLConqueror experiments used smaller or larger numbers of samples compared to SRS experiments. For these cases, we used order statistics (1/(n+1)) to derive if SPLConqueror performed better than SRS or not.

[13] SPLConqueror outperformed SRS in 7 points of BerkeleyDBC, 5 in 7z, and 0 in VP9, for 12-of-45=27%.

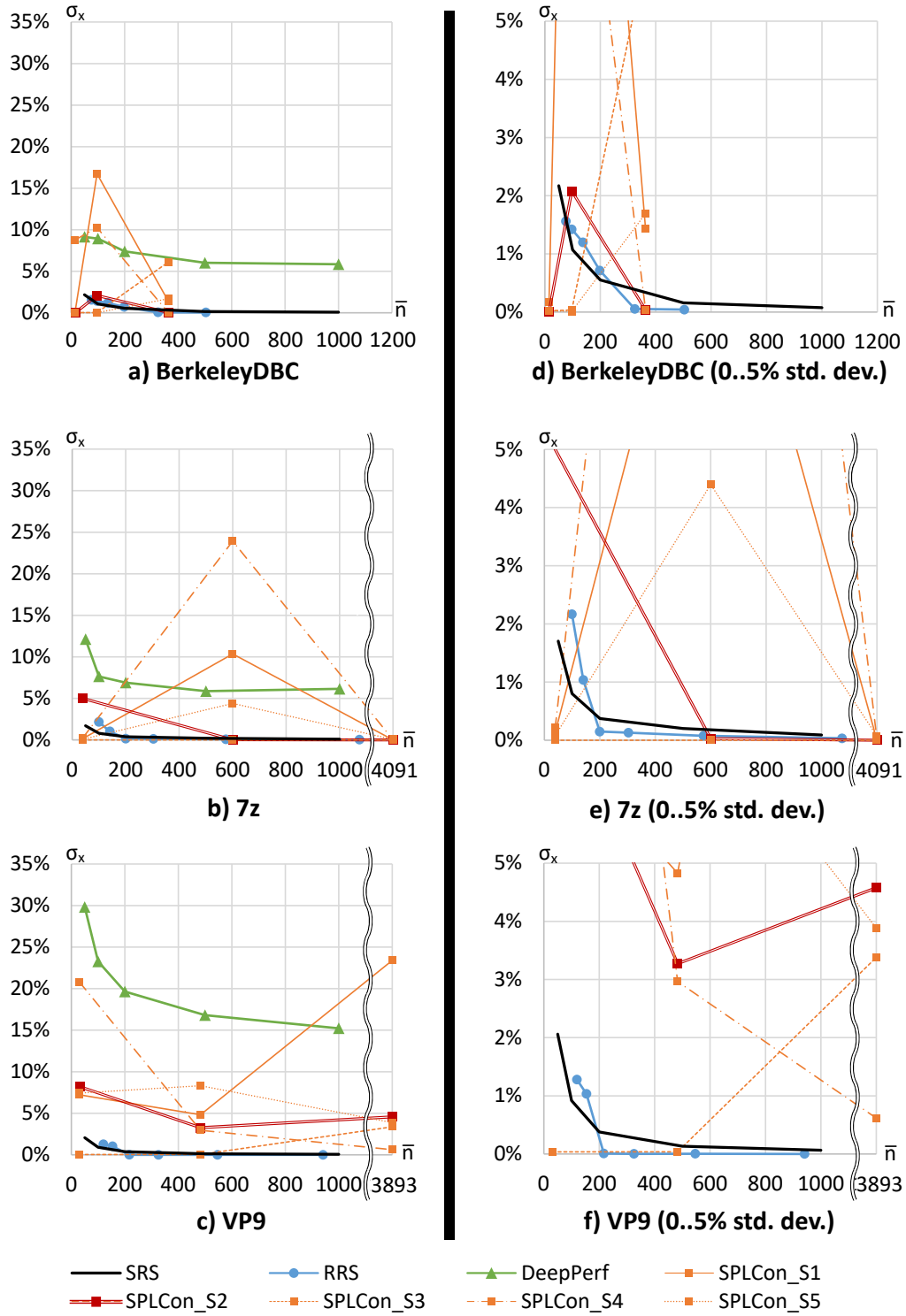

Fig. 14. Average Reliability (σ_x) *vs.* Average Sample Size ($\bar{n}$) by SPL and SPLO.

- SRS and RRS demonstrated consistently small σ_x below 1% for $\overline{n} \geq 200$ in all SPLs, matching the theoretical predictions of Fig. 5. Further the σ_x of SRS and RRS decreased steadily – well below 1% – as the sample size increased;
- When using ≥30 configs/recursion, the σ_x of μ_x is clearly lower for RRS than SRS (see Fig. 14b-c). Henceforth, we use MinSS=30 configurations per recursion unless otherwise specified.[10]
- DeepPerf reduced σ_x with increasing sample sizes up to 500; but not consistently over 500 (σ_x of 7z increased >500). Further DeepPerf has a significantly higher σ_x than SRS and RRS for all SPLs, doing no better than σ_x=6%.
- σ_x for SPLConqueror varies considerably. S3 and S5 had the lowest σ_x as it approached 0. The S3 and S5 PMs were created by samples from a SAT solver which is known to be biased [62]. We conjecture these PMs returned similar solutions. In general, larger sample sizes did not consistently lower σ_x and SPLConqueror σ_x were higher than those of SRS and RRS.
- The σ_x of SRS matches the theoretical σ_x for Order Statistics, Fig. 13(b). The SRS σ_x for 7z and VP9 measurements are slightly lower than theory Eqns (4)-(6) for the reason given earlier.

Conclusion: ***Sampling (esp. RRS) produced the lowest σ_x values and were the most reliable in these experiments.***

Additional Evidence. In [91], we compared a draft of RRS (here called RRS_0), with two PMs, one by Sarkar [101] and a precursor to SPLConqueror [106], on small SPLs explained earlier: Apache ($|\mathbb{C}|$=192), LLVM ($|\mathbb{C}|$=1024), and H264 ($|\mathbb{C}|$=1152). SRS dominated these PMs on all SPLs, and RRS_0 dominated SRS, consistent with results of this section.

5.4 RQ3: Are PM accuracy and PM solution accuracy correlated?

An implicit assumption in the SPL ML PM literature is "PM accuracy is correlated to PM solution accuracy" [42, 43, 106, 107, 109], which we call conjecture $\mathbb{K}$. To quantify $\mathbb{K}$, we use the *Mean Absolute Percentage Error* (MAPE), which is widely used as the overall measure of PM *accuracy* in SPL literature [42, 46]. MAPE is the average absolute difference between c's predicted performance $\hat{\$}(c)$ and c's benchmarked performance $\$(c)$. For an enumerable space $\mathbb{C}$:

$$\text{MAPE} = \frac{100}{|\mathbb{C}|} \cdot \sum_{c \in \mathbb{C}} \frac{|\$(c) - \hat{\$}(c)|}{\$(c)} \tag{12}$$

The box-plots[14] of Fig. 15a summarize MAPE values for the PMs obtained with DeepPerf and SPLConqueror. DeepPerf consistently produces more accurate and reliable PMs than SPLConqueror (*i.e.,* the boxes are nearer to the X-axis and narrower, respectively).

However, DeepPerf's predictions are not that good and worsen as $|\mathbb{C}|$ increases. Fig. 15b zooms MAPE values to DeepPerf's scale. DeepPerf's (a) *accuracy* decreases with increasing SPL size $|\mathbb{C}|$, as the median values are 3.7% (BerkeleyDBC), 9.7% (7z), and 17.5% (VP9) and (b) *reliability* also reduces with increasing SPL size $|\mathbb{C}|$, as the 25^{th} and 75^{th} percentiles are [2.6, 5.8] for BerkeleyDBC, [7.9, 19.0] for 7z, and [10.1, 44.0] for VP9. This suggests that although PMs for increasingly larger spaces can be created with small sample sizes, PM MAPE accuracy suffers.

The *solution accuracy* (β) of a PM is the rank of the c_{no} that it returns in an **RQ1** experiment. (Again, 100 such experiments were done per [PM, SPL, sample size] triplet). A (MAPE, β) pair can be defined for each PM per experiment. The scatter-plot in Fig. 16 shows the (MAPE, β) pairs collected from all **RQ1** experiments. Now conjecture $\mathbb{K}$: If MAPE and β are ideally correlated, there would be

[14] A *box-plot* encodes the values of five percentiles [121]. The bottom of the thin vertical line is the 0^{th} percentile (or lowest value); the top denotes the 100^{th} percentile (or highest value). The horizontal line in the box denotes the median; the box extends downwards to indicate 25^{th} percentile boundary and upwards the 75^{th} percentile boundary.

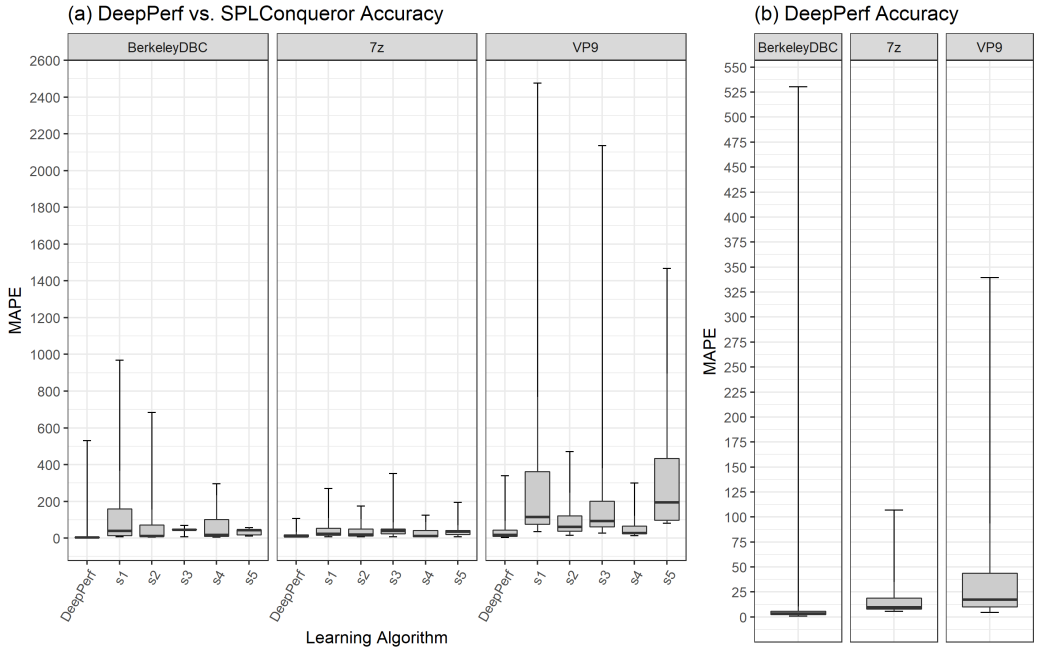

Fig. 15. MAPE accuracy of DeepPerf and SPLConqueror (S1-S5).

a 1-to-1 relationship between MAPE and β values; the points would follow a clear pattern, being aligned on a straight line or a curve. And if they were *positively* correlated, low MAPE values would correspond to low βs. If this is the case, an optimizer should return better c_{no}s with lower MAPE values.

Fig. 16 doesn't show this: DeepPerf in BerkeleyDBC displays a wide range of βs for the same MAPE values (*i.e.,* the points are vertically stacked). Inversely, for SPLConqueror S1 in VP9, PMs with very different MAPE values got roughly the same βs (*i.e.,* the points are horizontally aligned at different heights).

Table 6 lists the dependency between MAPE and β estimated with Spearman's ρ, Kendall's τ, Hoeffding's D [53], and Distance Correlation (dCor) [110]. The *magnitude* of these measures shows the strength of the dependency. The higher the magnitude, the more dependent are MAPE and β. A correlation measure c can be interpreted as *very weak* if $c<0.2$, *weak* if $0.2 \leq c < 0.4$, *moderate* if $0.4 \leq c < 0.6$, *strong* if $0.6 \leq c < 0.8$, and *very strong* if $c \geq 0.8$.

Algorithm	Correlation measure			
	Spearman's ρ	Kendall's τ	Hoeffding's D	dCor
DeepPerf	0.122	0.082	0.337	0.165
SPLCon. S1	0.214	0.131	0.345	0.229
SPLCon. S2	0.450	0.330	0.379	0.293
SPLCon. S3	0.443	0.323	0.370	0.342
SPLCon. S4	0.336	0.229	0.361	0.272
SPLCon. S5	0.559	0.420	0.433	0.783

Table 6. Correlation between MAPE and β for DeepPerf and SPLConqueror.

Note: The magnitude of ρ, τ, and dCor goes from 0 (no dependency) to 1 (total dependency), while D ranges from -0.5 (no dependency) to 1 (total dependency). To facilitate its comparison with the other measures, D was rescaled to [0..1]. Also, ρ and τ might have a negative *sign* if MAPE and β had an inverse relationship (β decreasing as MAPE increases), but this didn't occur.

Conclusion: ***An implicit assumption in ML PM literature is PM accuracy is correlated to PM solution accuracy. We found evidence to the contrary, as the correlation was weak in our experiments.***

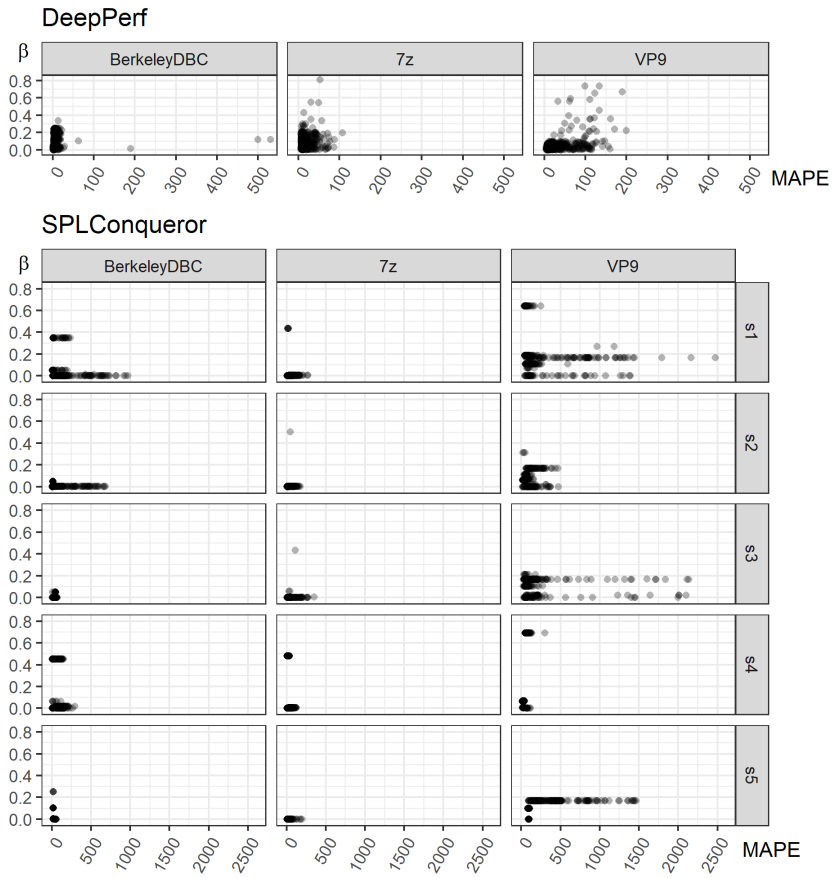

Fig. 16. PM accuracy (MAPE) and solution accuracy (β).

5.5 Threats to Validity

There are three confounding factors: SPLs, sample size, and graph shape.

- **SPLs.** We considered three enumerable SPLs whose sizes were ~10× larger than the next. Different performances might have resulted using other SPLs. However, SRS and RRS experimental results on an *additional three* enumerable SPLs in [91] (smaller than the SPLs used here) were consistent with this paper's results (see end of Sect. 5.3.)
- **Sample Size.** A goal or motivation of prior work was to use the smallest sample sizes possible to get accurate predictions. (Performance was the reason given in Sect. 3.3). We followed a standard evaluation procedure used in prior work to compare SRS and RRS with DeepPerf and SPLConqueror [46]. SRS and RRS consistently exhibited the smallest μ_x and smallest σ_x of c_{no}s returned across all sample sizes and SPLs considered. It is possible with larger sample sizes that DeepPerf and SPLConqueror might have performed better.
- **Graph Shape.** By chance, the three PCS graphs of enumerable SPLs, Fig. 11, are convex, *i.e.,* all have a gradual descent (from right to left) to the origin, c_{best}. Concave PCS graphs are harder to optimize. We delay further discussion of this topic, as Section 6 presents examples and the impact of concavity on optimization.

Research on ML PMs continues to advance, and so too their accuracy. The statements and results presented in this paper are state-of-the-art as of 2023.

5.6 Summary

SRS and RRS consistently produced the lowest ranked and most stable c_{no}s (*i.e.*, smallest μ_x and σ_x) across diverse enumerable SPLs of different sizes and sample sizes. We noticed in the ML PM literature an implicit assumption that a more accurate PM should produce more accurate c_{no}s, but the results of **RQ1** and **RQ2** suggested otherwise. Upon further investigation, we found the correlation of PM model accuracy is weak *w.r.t.* c_{no} (solution) accuracy. ***We again remind readers that we used a perfect optimizer to compute our PM results; an imperfect optimizer would unlikely improve PM performance.***

We offer an explanation for these results. Learning a function PM:$\mathbb{C}\rightarrow\mathbb{R}$ to predict the performance of every $c\in\mathbb{C}$ with MAPE accuracy $\leq$8% *and* $\mathbb{C}$ is colossal ($\gg 10^{10}$) *and* with sample sizes <5K is ***unbelievable***. ***ML PMs should do better with larger sample sizes, but this will be expensive. In contrast, finding near-optimals using a sample size <300 and be within 1% of optimal with 95% confidence in infinite-sized spaces is doable with sampling (see Table 3)***. Look carefully at Figs. 12-16 to see a recurring trend: as SPL size $|\mathbb{C}|$ increases, performance graphs become progressively more wild, meaning that the average accuracy and standard deviation of c_{no}s decrease with increasing $|\mathbb{C}|$ for the same sample sizes. And we learned that greater overall PM accuracy does ***not*** necessarily lead to better near-optimals. We are not optimistic that small sample sizes can produce truly accurate PMs for large SPL spaces. It is asking too much. Others, prior to us, reached a similar conclusion [128, 130].

Conclusion: ***Random sampling is a better technology match for SPLO than ML PMs.***

6 EVALUATION OF SRS AND RRS ON KCONFIG SPLS

We evaluate SRS and RRS on two SPLs that, to our knowledge, have not been evaluated in prior PM work *and* c_{no} estimates of c_{best} were found. Both use the Kconfig configuration tool [65]:

(1) axTLS 2.1.4 is a client-server library with 94 features and $2{\cdot}10^{12}$ configurations [11];

(2) ToyBox 0.7.5 is a Linux command line utilities package with 316 features and $1.4{\cdot}10^{81}$ configurations [112].

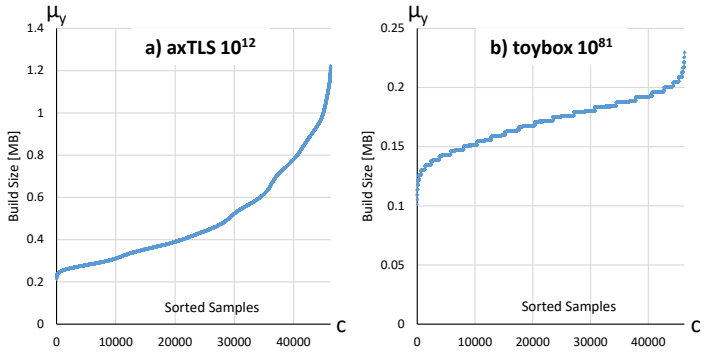

Fig. 17. PCS graph estimates using 200 configurations.

Both were benchmarked for their build size. Fig. 17 shows their minimum fidelity PCS graphs. We ask:

RQ4: Does RRS outperform SRS in colossal configuration spaces?

Unlike the SPLs from Section 5, we cannot measure the precise X-axis rank of configurations nor the value of c_{best} as both require enumeration. We can compare the true build size of solutions of SRS and RRS from the same SPL to determine the best c_{no}.

We devised an experiment to address **RQ4** so that it could be completed within two weeks:

- Compare SRS and RRS with the same total number of samples n = {100, 200, 300, 400, 500};
- SRS samples n configurations and reports the minimum build size;
- RRS samples MinSS=30 configurations per recursion;
- RRS terminates once the total number of configurations it uses reaches n, or by not finding a noteworthy feature, or when the constricted configuration subspace is smaller than 30 then enumeration occurs; and
- All experiments are repeated 25 times.

Fig. 18 shows the results.

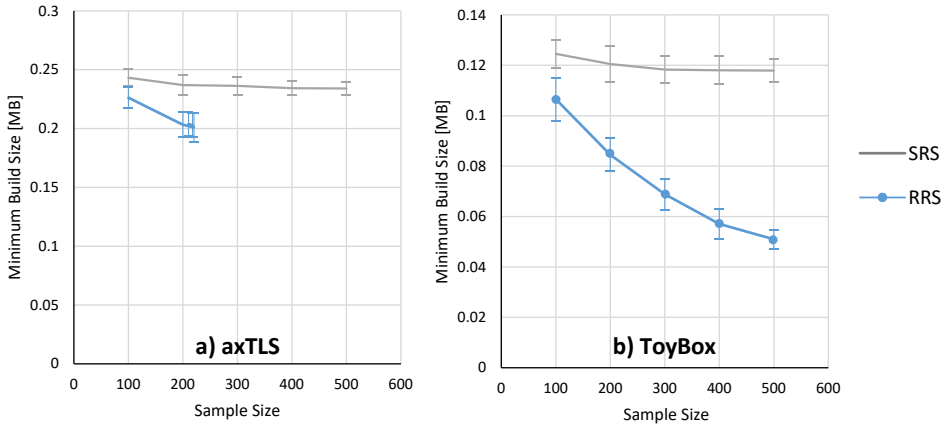

Fig. 18. Optimization of Kconfig SPLs using different sample sizes.

Observations. SRS generally found progressively better solutions as n increased for both axTLS and ToyBox; solutions for axTLS seemed to reach a fixed point when n>200.

RRS terminated early for axTLS for n∈{300, 400, 500}, where the average number of configurations benchmarked was 210, 217, 220. At termination, the last constricted space was so small that it was enumerated. The odd shape of Fig. 18a is simply RRS repeatedly converging on a near-minimum build size after examining >200 configurations. Overall, RRS found c_{nos} with smaller build sizes than SRS.

How good are these results? In an abandoned experiment prior to **RQ4**, we uniformly sampled and benchmarked 46250 configurations each from axTLS and ToyBox (included in our Zenodo download). We salvaged this work for **RQ4** as a 46250 point PCS graph, Fig. 20. The best solution had the percentile rank of $1/(46250+1)\cdot 100\% = .22\%$ or 5-sigma (≤.23%), a high level of resolution [98, 119]. We then overlaid the results of Fig. 18 and Fig. 20 to produce Fig. 21.

Fig. 21 magnifies Fig. 20 to the top-performing percentiles. PCS_{best} is the best-performing of all 46250 configurations. The dashed black line is the PCS_{best} boundary. With increasing sample sizes, SRS solutions approach PCS_{best}, as expected, but are never below PCS_{best}. RRS solutions appear as ✖s; they are literally inside the .22% percentile, visually on the Y-axis of each PCS graph usually below PCS_{best}. Overall, RRS solutions are better than PCS_{best} once n≥200.

On the Shape of PCS graphs. A key influence on SPLO is the shape of a PCS *near the origin*. There are two possibilities: a PCS graph is convex or concave, Fig. 19. The PCS graphs of enumerable SPLs, Fig. 11, are *convex*: they have a gradual slope to the origin where the *performance* (Y-axis) difference

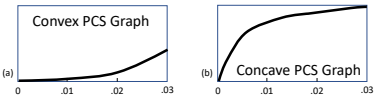

Fig. 19. Convex *vs.* Concave.

between 5%, 1%, and .05% percentile c_{no}s may not be much, and stopping a search sooner than .05% might seem acceptable.

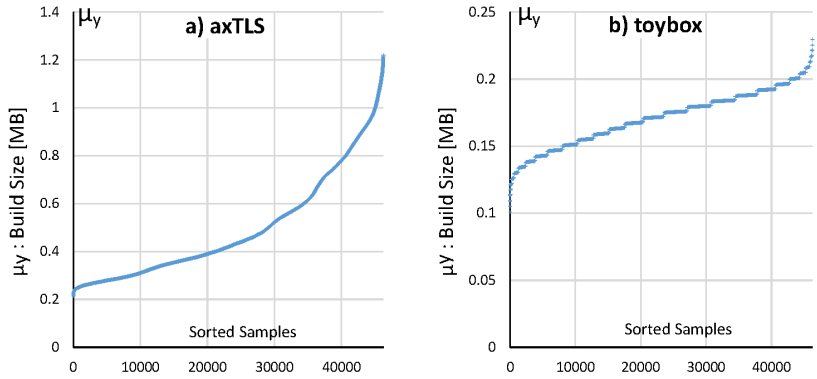

Fig. 20. Estimated PCS graphs using 46250 configurations.

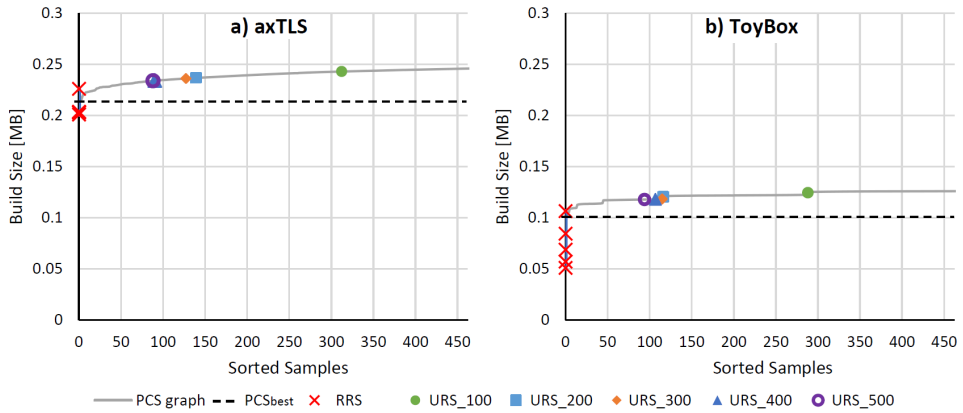

Fig. 21. Estimated PCS graphs, SRS and RRS results.

Concave PCS graphs are different: they have a steep drop to the origin. Concave graphs are harder to optimize, simply because the next round of sampling or recursion might produce a noticeably better c_{no}, so continued optimization is worth the effort. The 200-point PCS graph of ToyBox in Fig. 17b suggests concavity; not so for axTLS in Fig. 17a. However, their magnified (46250-point) PCS graphs in Fig. 21 confirm *both* are concave.

The dilemma is this: Generally, you don't know a priori whether a PCS graph is convex or concave near the origin until you look; there is no downside for continued searching if the allotment of configurations permits.

Conclusion: ***RRS finds better μ_y solutions than SRS. This has been a consistent result from small through colossal SPLs in our experiments.***

7 FIXED BUDGET SPLO: THE ESSENTIAL PROBLEM

Sections 5–6 compared different SPLO algorithms by averaging experiments that sampled tens of thousands of configurations per SPL. This extravagance is unlikely to be common in practice.

Instead, users are more likely to have a *fixed budget* (a maximum allotment of configurations for benchmarking) because of limited time, limited costs, *etc.* The challenge is that no single

SPLO algorithm will outperform all other algorithms for all SPLs or sample sizes. We know that RRS-is-always-better-than-SRS is false: there are cases in this paper where SRS performs better than RRS. But if a statistical bound on the quality of a solution is needed, SRS is the only game in town.

Here is a solution to the fixed budget SPLO: run ***both*** SRS and RRS with the same number of configurations. Both are executed in steps of N configurations, where N≥MinSS.

The first step samples N configurations using SRS. These samples are reused as the first N configurations of RRS. At this point, both SRS and RRS return the same "near optimal" configuration. In subsequent steps, SRS samples another N configurations from the entire space, while RRS samples a different set of N configurations from a noteworthy-constricted space. This last step is repeated until the allocation is exhausted. The best c_{no} returned by SRS or RRS is chosen, along with the statistical guarantees of the SRS c_{no}. SRS guarantees give a conservative bound on the goodness of the RRS c_{no}.

Example. Consider a budget of 450 configurations. The first 50 are used by both SRS and RRS; 400 configurations remain. 200 configurations are then allocated to both SRS and RRS, and are consumed in 4 additional rounds of 50 configurations each. A total of 450 configurations is consumed.

We repeated this 3 times, *i.e.*, we conducted 3 identical experiments (R1−R3) whose results are ***not*** averaged. Fig. 22 shows all three experiments return essentially the same result. Each red dot on the Y-axis indicates the first round results for both SRS and RRS for an experiment. Each red dot attached to two lines: one for SRS and the other for RRS.

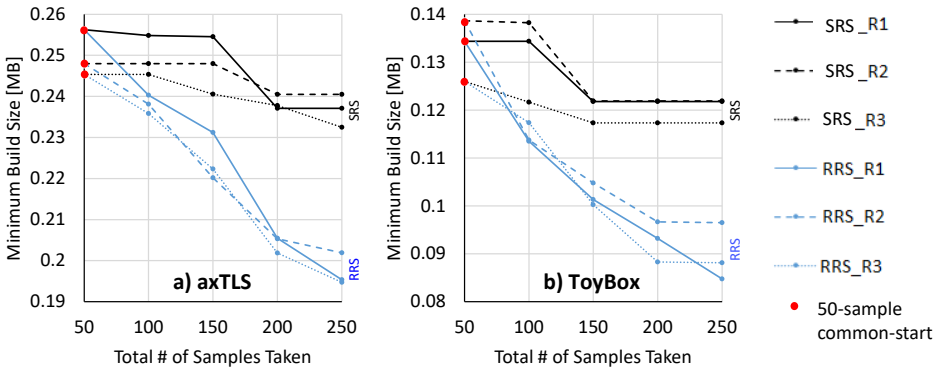

Fig. 22. Three examples of SRS and RRS using a Fixed Budget.

Table 7 tallies the results of (R1−R3). The c_{no} columns list the minimum build size found and "Best Alg" lists the algorithm that produced the solution. θ-Bound is a conservative theoretical bound on the goodness of the solution, derived from Eqn (8) using 250 configurations with 95% confidence yields 1.2% accuracy.

	axTLS $\lvert\mathbb{C}\rvert = 2 \cdot 10^{12}$		ToyBox $\lvert\mathbb{C}\rvert = 1.4 \cdot 10^{81}$	
Expr.	C_{no} [MB]	Best Alg.	C_{no} [MB]	Best Alg.
X1	0.195	RRS	0.085	RRS
X2	0.202	RRS	0.097	RRS
X3	0.195	RRS	0.088	RRS

θ-Bound = 1.2% accuracy at 95% confidence

Table 7. Results of fixed budget experiments.

Conclusion: ***Conclusion: A solution to the fixed budget SPLO problem gives the same number of configurations to SRS and RRS, and takes the best solution of the two. The statistical quality of the SRS solution serves as a conservative bound for RRS.***

8 RELATED AND FUTURE WORK

8.1 Highly Configurable Systems

Highly Configurable Systems (HCSs) define a broader universe in which SPLs and SPLO reside. HCSs have configuration parameters that are real and/or binary variables called *options* or *tuning knobs*. Unlike SPLs, an HCS has ***no*** feature model.

A pipeline of t tools is an example. Each tool has k (*e.g.*, command-line) options. Selecting any or all of the k options for a tool is possible, and selecting/deselecting an option for one tool has no effect on the selection or deselection of options of other tools. The configuration space size for this problem is precisely $2^{k \cdot t}$. HCSO, the HCS counterpart to SPLO, finds values for each of the $k \cdot t$ options that work best together for a given workload and environment [57].

Another example is a database system with w real-valued tuning knobs [7]. A space of $\mathbb{R}^w$ option combinations must be explored; the setting of one knob may trigger adjustments of other knobs. A challenge is to create ML models to understand the causal functional relationships among knobs [57]. HCSO finds a w-tuple that achieves a near-optimal performance [128, 130].

Yet another example is the *algorithm configuration* or *parameter tuning* problem [54], where the parameters of an algorithm are configured to achieve the algorithm's optimal performance for a given set of problem instances.

At a high abstraction level, HCSO and SPLO look alike. Unbeknown to us in 2003, Ye and Kalyanaraman developed an RRS-like algorithm (also named RRS) to search contour plots for minima in network parameter configurations [128]. They uniformly sampled an $\mathbb{R}^2$ space and used performance rankings to identify the top "noteworthy" 2D points. Then their RRS recursively drills down on areas surrounding these points to find minima. As there are no features (as in SPLs), the mechanisms of their RRS algorithm differ from ours. They also discovered Eqns (8)-(9) to guide their search and to choose sample sizes. Here again, their context and use of these equations differs from ours, but much is the same.

Fig. 23 is taken from [128]: the 2D contour is randomly sampled, and the top (in this case 3) performing regions in blue are "noteworthy" and RRS explores regions around these points.

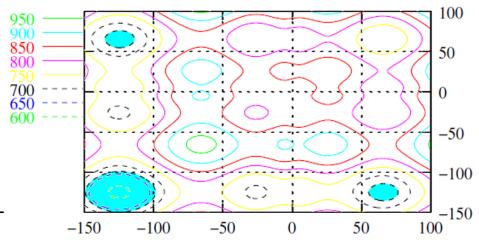

Fig. 23. Contours Explored Randomly.

The core differences between HCSs and SPLs are:

- HCSs have no feature model;
- Our SRS algorithm provides statistical guarantees on c_{nos} it returns. Order statistics are also useful and may be relevant to HCSO algorithms; and
- URS of SPL spaces is much harder as configurations are solutions to propositional formulas rather than points in continuous real 2D or n-D HCS spaces.

The rest of this section focuses on related work in the SPL domain.

8.2 Relevant Results in ML PMs

Other PMs for SPLOs. Guo *et al.* encoded a PM as a *Classification and Regression Tree* (CART) [43]. Sarkar *et al.* extended [43] with "projective sampling", a technique that checks performance-estimation accuracy improvement with more samples [101]. Later, Guo *et al.* improved the efficiency of CART by resampling and automated parameter tuning techniques [44].

Zhang *et al.* used Fourier learning and incrementally sampled configurations until a PM achieved a desired accuracy [129]. Ha *et al.* combined Fourier learning with LASSO regression to improve

the efficiency of learning Fourier coefficients for each feature [47]. Dorn *et al.* used probabilistic programming to derive a PM that captures the uncertainty from benchmarking configurations and reasoning with incomplete data [33]. Martin *et al.* compared different ML techniques and discovered that different methods work better for different SPLs and that feature selection techniques from ML can improve learning in general [80]. These papers were evaluated using relatively small SPLs with ≤60 features and |ℂ|≤250K. A survey of other PMs for configurable systems is in [1].

Scaling PMs. As of today, PMs of SPLs with $|\mathbb{C}|>10^6$ are rare. When attempted, a non-URS sample is taken whose size ranged from 500-5000 configurations, *i.e.,* the size of an enumerated SPL in this paper. Recently, PMs for Linux were created from 85K configurations [79]. Whether accurate PMs for colossal spaces can be learned from small samples ($85K \ll \sim 10^{4000}$) *and* be optimized efficiently is an interesting question beyond the scope of our paper.

Improving PM Accuracy. PMs are not very accurate [79, 115]. An SPL codebase can be carved into regions (methods or groups of methods) that have the same feature presence condition (*i.e.,* a feature qualification that must be satisfied for the region to be present in a product). By using fixed workloads and selecting configurations that cover (almost) all execution paths per region, a PM for each region is created. These PMs are then composed to produce a composite PM with improved accuracy.

Transfer Learning. A PM is created with a fixed workload. Should the workload change, the PM may need to be relearned (Section 2). An alternative is *transfer learning* [59]. Let $\hat{\$}:\mathbb{C}\rightarrow\mathbb{R}$ be the performance estimation function of a PM for space ℂ. A *transfer function* (TF) translates a $\hat{\$}$ learned for workload w to another function $\hat{\$}'$ with a different workload w′. A linear TF, $\hat{\$}'(c) = \alpha \cdot \hat{\$}(c) + \beta$, is postulated, ∀c∈ℂ. The values of constants α and β are learned. Linear TFs work well for small workload distortions, but existing evidence suggests otherwise for greater distortions [59, 79].

A recent paper by Martin *et al.* [79] presents a heterogeneous transfer learning method (tEAMS) that works surprisingly well to evolve PMs of progressive releases of Linux. MAPE values for newly learned PMs are in the 8.2%-9.2% range. When using the same budget, tEAMS produces transferred PMs with MAPE values 5.6%-7.1%. However, MAPE values tend to degrade after multiple transfers.

8.3 Optimizers

Optimizers for SPLs. Optimizers in the SPLO literature have focused on *multi-objective optimization* using evolutionary algorithms [32, 68, 127], active learning [131], filtered Cartesian flattening [117, 118], and integer programming [127]. Two other tools known to us used PMs specifically to learn near-optimals: rank-learners [87] and FLASH [88].

Nair *et al.* observed experimentally that PM accuracy improves rapidly as more configurations are used to train them. A point is eventually reached where improvement stagnates, and it is wasteful to use additional configurations. The stagnation point can be detected by measuring if the accuracy of PM trained with more additional configurations differs substantially (*e.g.,* computing the MAPE difference between PMs). Nair *et al.* claim that comparing PMs ability to rank configurations instead of their accuracy is a better stopping criterion that detects the stagnation point earlier *and* with the goal of returning good near-optimal configurations. Experiments show their rank stopping criterion sometimes saves configurations, but Fig. 7 in [87] says it gets slightly worse rankings than conventional non-ranked approaches.

FLASH is a follow-on paper by the same authors. It relies on *Sequential Model-Based Optimization* [56], a broad generalization of RRS for HCSO. To optimize a performance metric, FLASH builds a CART model with an initial learning set L of benchmarked configurations. Then another set S of

configurations is chosen, CART estimates the performance of each $s \in S$, and the best-performing configuration, c_{no}, from S is returned. This c_{no} is then benchmarked, added to L, and this cycle repeats for a budgeted number of iterations. FLASH was evaluated on tiny (<6 options w. $|\mathbb{C}|<4K$) and small (<20 options w. $|\mathbb{C}|<240K$) HCSs.

In both of these papers, no statistical guarantees (within x% of optimal with y% confidence) are returned, which we feel is essential for optimization.

Domain-Specific Optimizers. Exploiting domain-specific knowledge can lead to better c_{no}s. COZART [72] is a tool to find a Linux kernel configuration with minimum build size. With prior knowledge of which features are necessary for booting the Linux kernel and that build size decreases by deselecting features, COZART derives a configuration that selects the necessary features and excludes others as much as possible. COZART does not search for configurations, yet it finds a configuration smaller than sampling does.

Random Search Optimizers. *Random Search* is a family of numerical optimization algorithms for functions that are discontinuous and non-differentiable [18, 123]. SRS and RRS are examples. There is nothing preventing SRS or RRS to be used as an optimizer for a PM: replace the component that builds a configuration c and benchmarks it, with a component that calls a PM to return an estimate of c's performance. The inaccuracy of PM predictions may limit the utility of statistical guarantees of SRS.

8.4 Sampling SPL Configurations

As late as 2020, it was believed that URS of non-enumerable SPL spaces was infeasible [62, 97]. Consequently, novel sampling algorithms were proposed as substitutes. Dutra *et al.* devised QuickSampler which randomly selects features to form a configuration and attempts to fix the configuration using a MaxSAT solver [34], a solver that tries to maximize the number of satisfiable CNF clauses. Kaltenecker *et al.* introduced *Diversified Distance-based Sampling* (DDbS) which treats configurations as vectors and derives configurations with maximum difference among them [62]. MaxSAT (and thus QuickSampler) does not achieve URS and DDbS is not scalable [92]. Many more are cited in [1].

Some build tools offer their own sampling algorithm. Kconfig [65] has the conf tool [36], that has the randconfig option to randomly generate configurations that are not uniform. randconfig assigns values to features in the order they appear in a Kconfig specification, so that a valid value for a feature being examined may be constrained by the selection of prior features. Samples are therefore biased. Recently, another tool called KconfigSampler [37] supports the *hierarchical random sampling* of the Linux Kernel. This kind of sampling is not uniform but ensures that features at the same abstraction level in the Kconfig specification have the same probability of appearing in a random configuration. KconfigSampler is implemented as a net of interconnected BDDs.

Other tools partition the solution space into cells as evenly as possible using universal hashing functions. Then, the tool selects one cell at random, and generates a solution with a SAT solver. UniWit [26] was the first sampler to implement this idea, which guaranteed uniformity but has serious scalability limitations. Two later iterations of UniWit, called Unigen [28] and Unigen2 [25], tried to improve scalability while keeping uniformity, with not much success [51, 97]. The last UniWit iteration is UniGen3 [76], which finally sacrifices uniformity to provide scalability.

Other work achieved URS by counting solutions of a propositional formula ϕ. Oh *et al.* were first to experimentally demonstrate URS of large SPL spaces. They used a model counting BDD to count the exact number of solutions to ϕ and functionality-constrained versions of ϕ [91]. This work was later generalized with the Smarch tool, which uses #SAT and Alg. 1, Section 3.3.

Three other samplers based on counting are Spur [5], KUS [102], and BDDSampler [50]. Spur relies on #SAT technology, KUS on a knowledge compilation structure called *Deterministic Decomposable Negation Normal Form* (d-DNNF), and BDDSampler on BDDs. The evaluation of Unigen2, Smarch, Spur, KUS, and BDDSampler was reported in [50]; a variety of models, in terms of size (from 14 to 18,570 variables) and application domain (automotive industry, embedded systems, a laptop customization system, a web application generator, integrated circuits, etc.) were examined. Results showed that only BDDSampler currently provides both uniformity and scalability.

8.5 Feature Models and URS

Numerical Features. This paper focused on binary {0,1} features to match classical SPL feature models [9, 14]. However, the Linux build tool Kconfig [64] has feature models with binary and *numerical features* (NFs). An NF is a numerical value within a bounded range, which can be approximated by an integer in a corresponding range. *Bit-blasting* is a technique to encode numerical values as bit vectors and arithmetic operations and constraints as propositional formulas [24]. This allows NF propositional formulas to be directly analyzed "as is" by both SRS and RRS [83, 84]. As DeepPerf and SPLConqueror can handle NFs natively, future work should compare how SRS and RRS perform *w.r.t.* DeepPerf, SPLConqueror, and FLASH on NF models.

Scalability of URS. Our analysis of URS, Eqns (2)-(9), yields results for an infinite-sized configuration space. However, the best tools today [17] cannot analyze Linux, the largest known SPL, whose estimated size exceeds 10^{2200}. Extending today's #SAT and BDD technologies to analyze Linux remains a challenge.

Dimension Reduction. Not all features contribute to performance; most features of an SPL are of this type. There are several ways in which irrelevant features can be identified and removed from ML PMs [4, 46, 107].

SRS and RRS do something similar: they ignore non-noteworthy features. In contrast, how performance-irrelevant features can be eliminated from a feature model's propositional formula ϕ *and* still admit model counting is not obvious. If this could be done, it might solve the scalability problems that remain for URS, discussed above.

Tseitin's Transformation. Not any translation of a feature model to propositional formula ϕ and then to a CNF formula, ϕ^{cnf}, can be used with a #SAT sampling tool. Some translations do not preserve the 1:1 correspondence between products and solutions of ϕ, resulting in an overcounting. Tseiten's transformation is one of several transformations that preserves the required 1:1 correspondence for URS [113]. The check: if a translation of ϕ to ϕ^{cnf} adds no additional variables (features), then $|\mathbb{C}|=|\phi^{cnf}|$. BDDs do not have this problem. See Appendix D for more details.

RRS *vs.* SRS. A perfect RRS would constrain $\mathbb{C}$ in each recursive iteration by selecting a subspace that *always* contains c_{best}. Currently, RRS uses a heuristic that chooses noteworthy features with the best contributing performance in a sample. This procedure works most times, but as we saw not always. An open problem remains: is there an improved RRS algorithm or analysis that always selects a subspace containing c_{best} with a computable degree of confidence?

9 CONCLUSIONS

ML is an alluring way to explore PMs for SPLs. But lacking a scalable way to uniformly sample highly-constrained spaces of colossal ($\gg 10^{10}$) SPLs had two consequences. (1) Serious efforts were spent on non-URS methods to find substitutes for URS [1, 3, 25, 27, 34, 42, 49, 62, 65], but to properly evaluate their statistical behavior, a gold standard required URS. (2) Most PMs were not adequately

evaluated for scalability; SPLs with enumerable spaces (≤250K) were common until recently (*e.g.*, [79]). In Sect. 3.3, we diminished these problems by showing how to uniformly sample colossal SPL configuration spaces as large as 10^{1441}.

An initial motivation for PMs was to find SPL c_{no}s for a given workload. Typical PMs required an optimizer to find a c_{no}; but the only way to determine the quality of c_{no}s (*e.g.*, how near they are to optimal) required enumerable SPLs. In Sects. 3.1–3.2, we showed how order statistics with URS provided a needed statistical guarantee for colossal SPLs: a c_{no} is within x% of optimal with y% confidence. Further, given any two of (accuracy x%, confidence y%, or sample size n) for a c_{no}, the third is computed by an equation or found in a table.

Two random search algorithms that used URS were presented, SRS and RRS. With enumerated SPLs in Sect. 5, we compared them to state-of-the-art PMs, DeepPerf (a sparse neural network) and SPLConqueror (linear regression), on c_{no} accuracy (average distance μ from optimal) and reliability (standard deviation of μ). Experiments showed SRS dominated both PMs, and RRS dominated SRS. Further, a common belief in the PM literature is "a more accurate PM produces a more accurate c_{no}". We found evidence to the contrary, where PM accuracy was weakly correlated to c_{no} accuracy.

In Sect. 6, we demonstrated the efficacy of RRS and SRS on two colossal SPLs: axTLS ($|\mathbb{C}|=10^{12}$) and ToyBox ($|\mathbb{C}|=10^{81}$). Sampling at most 500 configurations, RRS found c_{no}s that were inside .22 percentile (or 5-sigma) of optimal for both SPLs. And in Sect. 7, we presented a fixed budget algorithm that gave the same sample size to both RRS and SRS, let each compute their c_{no}s where the best c_{no} was returned along with the statistical guarantees of SRS, as RRS has no guarantees.

Our work encourages further research on topics of substance: (1) generalize URS to numerical features; (2) compare PMs with SRS and RRS on numerical feature models; (3) use URS to determine how well PMs scale to colossal SPLs; and (4) improve URS scalability to the largest known SPL: the Linux Kernel.

Acknowledgments. We thank the referees for their help to improve this paper. We also thank Prof. Marijn Heule (CMU), Daniel-Jesus Munoz (U. of Malaga), Prof. Maggie Myers (UT Austin), and Prof. Norbert Siegmund (U. Liepzig). Work by Oh and Batory was supported by NSF grants CCF1212683 and ACI-1550493. Work by Heradio was supported by the Universidad Nacional de Educacion a Distancia (projects 2021V/PUNED/008 and 2022V/PUNED/007).

REFERENCES

[1] 2021. Learning software configuration spaces: A systematic literature review. *JSS* 182 (2021).
[2] 7z Website 2021. 7z Website. https://www.7-zip.org/download.html.
[3] M. Acher et al. 2019. *Learning Very Large Configuration Spaces: What Matters for Linux Kernel Sizes.* Technical Report hal-02314830. Inria Rennes.
[4] M. Acher et al. 2022. Feature Subset Selection for Learning Huge Configuration Spaces: the Case of Linux Kernel Size. In *SPLC*.
[5] D. Achlioptas, Z.S. Hammoudeh, and P. Theodoropoulos. 2018. Fast Sampling of Perfectly Uniform Satisfying Assignments. In *SAT*.
[6] S. Agrawal, S. Chaudhuri, and V. Narasayya. 2000. Automated Selection of Materialized Views and Indexes in SQL Databases. In *VLDB*.
[7] D. Van Aken, A. Pavlo, G.J. Gordon, and B. Zhang. 2017. Automatic Database Management System Tuning Through Large-Scale Machine Learning. In *SIGMOD*.
[8] Apache Web Server 2002. Apache HTTP Server Project. https://httpd.apache.org/.
[9] S. Apel, D. Batory, C. Kästner, and G. Saake. 2013. *Feature-Oriented Software Product Lines.* Springer.
[10] B.C. Arnold, N. Balakrisnhan, and H.N. Nagaraja. 2008. *A First Course in Order Statistics.* SIAM.
[11] axTLS 2018. AxTLS Website. http://axtls.sourceforge.net/.
[12] R.A. Aziz, G. Chu, C.J. Muise, and P.J. Stuckey. 2015. #∃SAT: Projected Model Counting. In *SAT*.
[13] D. Batory. 2005. Feature Models, Grammars, and Propositional Formulas. In *SPLC*.
[14] D. Batory. 2021. *Automated Software Design: Volume 1.* Lulu Press.

[15] D. Batory and C. Gotlieb. 1982. A Unifying Model of Physical Databases. *ACM TODS* (Dec. 1982).
[16] D. Batory, J. Oh, R. Heradio, and D. Benavides. 2021. Product Optimization in Stepwise Design. In *Logic, Computation and Rigorous Methods*, A. Raschke, E. Riccobene, and K.D. Schewe (Eds.). Springer.
[17] BDDSampler 2022. BDDSampler Website. https://github.com/davidfa71/BDDSampler.
[18] J. Bergstra and Y. Bengio. 2012. Random Search for Hyper-Parameter Optimization. *JMLR* (2012).
[19] BerkeleyDB Website 2021. BerkeleyDB Website. https://www.oracle.com/database/technologies/related/berkeleydb.html.
[20] A. Biere, M. Heule, H. Maaren, and T. Walsh. 2009. *Handbook of Satisfiability: Volume 185 Frontiers in Artificial Intelligence and Applications*. IOS Press.
[21] A. Bluman. 2009. *Elementary Statistics: A Step by Step Approach*. McGraw-Hill Higher Education.
[22] L. Breiman, J. Friedman, R. Olshen, and C. Stone. 1984. *Classification and Regression Trees*. Wadsworth and Brooks/Cole Advanced Books and Software.
[23] P. Bruce, A. Bruce, and P. Gedeck. 2020. *Practical Statistics*. O'Reilly.
[24] R. Bryant et al. 2007. Deciding Bit-vector Arithmetic with Abstraction. In *TACAS*.
[25] S. Chakraborty, D.J. Fremont, K.S. Meel, S.A. Seshia, and M.Y. Vardi. 2015. On Parallel Scalable Uniform SAT Witness Generation. In *TACAS*.
[26] S. Chakraborty, K.S. Meel, and M.Y. Vardi. 2013. A Scalable and Nearly Uniform Generator of SAT Witnesses. In *CAV*.
[27] S. Chakraborty, K. Meel, and M. Vardi. 2013. A Scalable Approximate Model Counter. In *CP*.
[28] S. Chakraborty, K.S. Meel, and M.Y. Vardi. 2014. Balancing Scalability and Uniformity in SAT Witness Generator. In *DAC*.
[29] S. Chaudhuri. 1998. An Overview of Query Optimization in Relational Systems. In *PODS*.
[30] T.Y. Chen, H. Leung, and I.K. Mak. 2004. Adaptive Random Testing. In *ASIAN*.
[31] CUDD Website 2022. CUDD Website. https://github.com/vscosta/cudd.
[32] K. Deb, A. Pratap, S. Agarwal, and T. Meyarivan. 2002. A Fast and Elitist Multiobjective Genetic Algorithm: NSGA-II. *IEEE TEVC* (April 2002).
[33] J. Dorn, S. Apel, and N. Siegmund. 2020. Mastering Uncertainty in Performance Estimations of Configurable Software Systems. In *ASE*.
[34] R. Dutra, K. Laeufer, J. Bachrach, and K. Sen. 2018. Efficient Sampling of SAT Solutions for Testing. In *ICSE*.
[35] D. Fernandez-Amoros, S. Bra, E. Aranda-Escolastico, and R. Heradio. 2020. Using Extended Logical Primitives for Efficient BDD Building. https://www.mdpi.com/2227-7390/8/8/1253. *Mathematics* 8, 8 (2020), 1–17.
[36] D. Fernandez-Amoros, R. Heradio, C. Mayr-Dorn, and A. Egyed. 2019. A Kconfig translation to logic with one-way validation system. In *SPLC*.
[37] D. Fernandez-Amoros, R. Heradio, C. Mayr-Dorn, and A. Egyed. 2022. Scalable Sampling of Highly-Configurable Systems: Generating Random Instances of the Linux Kernel. In *ASE*.
[38] A. Field, J. Miles, and Zoë Field. 2012. *Discovering Statistics Using R*. SAGE Publications LTD.
[39] P. Gazillo, J. Oh, and M. Myers. 2019. *Uniform Sampling from Kconfig Feature Models*. Technical Report TR-19-02. University of Texas at Austin, Department of Computer Science.
[40] V. Gogate and R. Dechter. 2006. A New Algorithm for Sampling CSP Solutions Uniformly At Random. In *CP*.
[41] J. Guo et al. 2017. SMTIBEA: a Hybrid Multi-objective Optimization Algorithm for Configuring Large Constrained Software Product Lines. *SoSyM* (2017), 1–20.
[42] J. Guo et al. 2018. Data-efficient Performance Learning for Configurable Systems. *Empirical Software Engineering* 23, 3 (2018), 1826–1867.
[43] J. Guo, K. Czarnecki, S. Apel, N. Siegmund, and A. Wasowski. 2013. Variability-aware Performance Prediction: A Statistical Learning Approach. In *ASE*.
[44] J. Guo and K. Shi. 2018. To Preserve Or Not to Preserve Invalid Solutions in Search-bassed Software Engineering: A Case Study in Software Produce Lines. In *ICSE*.
[45] H.264 Video Compression 2022. H.264 Video Compression. https://www.haivision.com/resources/streaming-video-definitions/h-264/.
[46] H. Ha and H. Zhang. 2019. Deepperf: Performance Prediction for Configurable Software with Deep Sparse Neural Network. In *ICSE*.
[47] H. Ha and H. Zhang. 2019. Performance-Influence Model for Highly Configurable Software with Fourier Learning and Lasso Regression. In *ICSME*.
[48] A. Halin, A. Nuttinck, M. Acher, X. Devroey, G. Perrouin, and B. Baudry. 2019. Test Them All, Is It Worth It? Assessing Confguration Sampling on the JHipster Web Development Stack. *Empirical Software Engineering* (April 2019).
[49] C. Henard, M. Papadakis, M. Harman, and Y. Traon. 2015. Combining Multi-objective Search and Constraint Solving for Configuring Large Software Product Lines. In *ICSE*.

[50] R. Heradio et al. 2022. Uniform and Scalable Sampling of Highly Configurable Systems. *Empirical Software Engineering* 27, 2 (2022), 44.
[51] R. Heradio, D. Fernandez-Amoros, J.A. Galindo, and D. Benavides. 2020. Uniform and Scalable SAT-Sampling for Configurable Systems. In *SPLC)*.
[52] M.J. Heule, O. Kullmann, S. Wieringa, and A. Biere. 2011. Cube and Conquer: Guiding CDCL SAT Solvers by Lookaheads. In *HVC*.
[53] W. Hoeffding. 1948. A Non-parametric Test of Independence. *Annals of Mathematical Statistics* 19, 4 (1948), 546–557.
[54] H.H. Hoos. 2012. *Automated Algorithm Configuration and Parameter Tuning*.
[55] J.M. Horcas, M. Pinto, and L. Fuentes. 2018. Variability Models for Generating Efficient Configurations of Functional Quality Attributes. *Information and Software Technology* 95 (2018), 147–164.
[56] F. Hutter, H.H. Hoos, and K. Leyton-Brown. 2011. Sequential Model-Based Optimization for General Algorithm Configuration. In *LION*.
[57] M.S. Iqbal, R. Krishna, M.A. Javidian, B. Ray, and P. Jamshidi. 2022. Unicorn: Reasoning About Configurable System Performance Through the Lens of Causality. In *EuroSys*.
[58] P. Jackson and D. Sheridan. 2004. Clause Form Conversions for Boolean Circuits. In *SAT*.
[59] P. Jamshidi et al. 2017. Transfer Learning for Performance Modeling of Configurable Systems: An Exploratory Analysis. In *ASE*.
[60] P. Jamshidi and G. Casale. 2016. An Uncertainty-aware Approach to Optimal Configuration of Stream Processing Systems. In *MASCOTS*.
[61] M. Järvisalo, A. Biere, and M.J.H. Heule. 2010. Blocked Clause Elimination. In *TACAS*.
[62] C. Kaltenecker, A. Grebhahn, N. Siegmund, J. Guo, and S. Apel. 2019. Distance-Based Sampling of Software Configuration Spaces. In *ICSE*.
[63] M. Karnaugh. 1953. The Map Method for Synthesis of Combinational Logic Circuits. *IEEE Communication and Electronics* 72, 5 (1953).
[64] Kconfig Language 2018. Kconfig Language Specification. https://www.kernel.org/doc/Documentation/kbuild/kconfig-language.txt.
[65] Kconfig Tool 2018. Kconfig Tool Specification. https://www.kernel.org/doc/Documentation/kbuild/kconfig.txt.
[66] D.E. Knuth. 2009. *The Art of Computer Programming, Volume 4, Fascicle 1: Bitwise Tricks & Techniques, Binary Decision Diagrams*. Addison-Wesley Professional.
[67] S. Kolesnikov, N. Siegmund, C. Kästner, A. Grebhahn, and S. Apel. 2019. Tradeoffs in Modeling Performance of Highly Configurable Software Systems. *SoSyM* 18, 3 (2019), 2265–2283.
[68] J. Krall, T. Menzies, and M. Davies. 2015. Gale: Geometric Active Learning for Search-Based Software Engineering. *IEEE TSE* (Oct. 2015).
[69] S. Krieter. 2019. Enabling Efficient Automated Configuration Generation and Management. In *SPLC*.
[70] W. Kruskal. 1952. Use of ranks in one-criterion variance analysis. *J. Amer. Statist. Assoc.* 47, 260 (1952), 583–621.
[71] O. Kullmann. 1999. On a Generalization of Extended Resolution. *Discrete Applied Mathematics* 96-97 (1999), 149 – 176.
[72] H. Kuo, J. Chen, S. Mohan, and T. Xu. 2020. Set the Configuration for the Heart of the Os: On the Practicality of Operating System Kernel Debloating. *POMACS* 4, 1 (2020), 1–27.
[73] B. Lantz. 2019. *Machine Learning with R*. Packt Publishing.
[74] H. Levene. 1960. *Robust tests for equality of variances*. Stanford University Press.
[75] LLVM 2020. The LLVM Compiler Infrastructure. https://llvm.org/.
[76] S. Gocht M. Soos and K.S. Meel. 2020. Tinted, Detached, and Lazy CNF-XOR solving and its Applications to Counting and Sampling. In *CAV*.
[77] Mann Whitney 2020. Mann-Whitney U-Test (Wilcoxon Rank Sum Test). https://sphweb.bumc.bu.edu/otlt/mph-modules/bs/bs704_nonparametric/BS704_Nonparametric4.html.
[78] B. Marker, D. Batory, and R. Geijn. 2014. Understanding Performance Stairs: Elucidating Heuristics. In *ASE*.
[79] H. Martin et al. 2021. Transfer Learning Across Variants and Versions: The Case of Linux Kernel Size. *IEEE TSE* (Sept. 2021).
[80] H. Martin, M. Acher, J.A. Pereira, and J. Jézéquel. 2021. A Comparison of Performance Specialization Learning for Configurable Systems. In *SPLC*.
[81] MathIsFun.com. 2019. Standard Deviation Formulas. https://www.mathsisfun.com/data/standard-deviation-formulas.html.
[82] F. Medeiros, C. Kästner, M. Ribeiro, R. Gheyi, and S. Apel. 2016. A Comparison of 10 Sampling Algorithms for Configurable Systems. In *ICSE*.

[83] D. Munoz, J. Oh, M. Pinto, L. Fuentes, and D. Batory. 2019. Uniform Random Sampling Product Configurations of Feature Models That Have Numerical Features. In *SPLC*.

[84] D. Munoz, J. Oh, M. Pinto, L. Fuentes, and D. Batory. 2022. Nemo: A Tool to Transform Feature Models with Numerical Features and Arithmetic Constraints. In *ICSR*.

[85] D.J. Munoz, M. Pinto, and L. Fuentes. 2018. Finding Correlations of Features Affecting Energy Consumption and Performance of Web Servers Using the HADAS Eco-assistant. *Computing* 100, 11 (Nov. 2018), 1155–1173.

[86] S. Muroga. 1979. *Logic Design and Switching Theory.* John Wiley & Sons, Inc.

[87] V. Nair, T. Menzies, N. Siegmund, and S. Apel. 2017. Using Bad Learners to Find Good Configurations. In *FSE*.

[88] V. Nair, Z. Yu, T. Menzies, N. Siegmund, and S. Apel. 2020. Finding Faster Configurations Using FLASH. *IEEE TSE* (July 2020).

[89] A. Nöhrer and A. Egyed. 2013. C2O Configurator: a Tool for Guided Decision-making. In *ASE*.

[90] J. Oh. 2022. *Finding Near-Optimal Configurations in Colossal Product Spaces of Highly Configurable Systems.* Ph. D. Dissertation. University of Texas at Austin, Dept. of Computer Science.

[91] J. Oh, D. Batory, M. Myers, and N. Siegmund. 2017. Finding Near-optimal Configurations in Product Lines by Random Sampling. In *FSE*.

[92] J. Oh, P. Gazzillo, D. Batory, M. Heule, and M. Myers. 2020. *Scalable Uniform Sampling for Real-World Software Product Lines.* Technical Report TR-20-01. Dept. of Computer Science, University of Texas at Austin.

[93] R. Olaechea, D. Rayside, J. Guo, and K. Czarnecki. 2014. Comparison of Exact and Approximate Multi-objective Optimization for Software Product Lines. In *ICSE*.

[94] J. Pereira, M. Acher, H. Martin, and J.M. Jézéquel. 2020. Sampling Effect on Performance Prediction of Configurable Systems: A Case Study. In *ICPE*.

[95] P. Perrotta. 2020. *Programming Machine Learning: From Coding to Deep Learning.* The Pragmatic Bookshelf.

[96] D.A. Plaisted and S. Greenbaum. 1986. A Structure-preserving Clause Form Translation. *Symbolic Computation* 2, 3 (1986), 293 – 304.

[97] Q. Plazar, M. Acher, G. Perrouin, X. Devroey, and M. Cordy. 2019. Uniform Sampling of SAT Solutions for Configurable Systems: Are We There Yet?. In *ICST*.

[98] T. Puiu. 2021. What Does 5-sigma Mean in Science? https://www.zmescience.com/science/what-5-sigma-means-0423423/.

[99] J.P. Royston. 1982. An Extension of Shapiro and Wilk's W Test for Normality to Large Samples. *Journal of the Royal Statistical Society* 31, 2 (1982), 115–124.

[100] L.E. Sánchez, J.A. Diaz-Pace, and A. Zunino. 2019. A Family of Heuristic Search Algorithms for Feature Model Optimization. *Science of Computer Programming* 172 (2019), 264 – 293.

[101] A. Sarkar, J. Guo, N. Siegmund, S. Apel, and K. Czarnecki. 2015. Cost-efficient Sampling for Performance Prediction of Configurable Systems. In *ASE*.

[102] S. Sharma, R. Gupta, S. Roy, and K.S. Meel. 2018. Knowledge Compilation Meets Uniform Sampling. In *LPAR*.

[103] K. Shi. 2017. Combining Evolutionary Algorithms with Constraint Solving for Configuration Optimization. In *ICSME*.

[104] S. Siegel and J. Castellan. 1988. *Nonparametric Statistics for the Behavioral Sciences.* MacGraw Hill.

[105] N. Siegmund et al. 2012. Dataset for Siegmund2012. http://fosd.de/SPLConqueror.

[106] N. Siegmund et al. 2012. Predicting Performance Via Automated Feature-interaction Detection. In *ICSE*.

[107] N. Siegmund, A. Grebhahn, S. Apel, and C. Kästner. 2015. Performance-Influence Models for Highly Configurable Systems. In *FSE*.

[108] N. Siegmund, M. Rosenmüller, M. Kuhlemann, C. Kästner, and G. Saake. 2012. SPL Conqueror: Toward Optimization of Non-functional Properties in Software Product Lines. *Software Quality Journal* (Sept. 2012).

[109] N. Siegmund, S. Sobernig, and S. Apel. 2017. Attributed Variability Models: Outside the Comfort Zone. In *FSE*.

[110] G.J. Székely, M.L. Rizzo, and N.K. Bakirov. 2007. Measuring and Testing Dependence by Correlation of Distances. *The Annals of Statistics,* 35, 6 (2007), 27692794.

[111] M. Thurley. 2006. SharpSAT–counting Models with Advanced Component Caching and Implicit BCP. In *SAT*.

[112] Toybox 2018. Toybox Website. http://landley.net/toybox/.

[113] G.S. Tseitin. 1983. On the Complexity of Derivation in Propositional Calculus. In *Automation of Reasoning*, J. Wrightson et al. (Eds.).

[114] S. Vasishth and M. Broe. 2011. *The Foundations of Statistics: A Simulation-based Approach.* Springer Berlin, Heidelberg.

[115] M. Velez, P. Jamshidi, N. Siegmund, S. Apel, and C. Kästner. 2021. White-Box Analysis Over Machine Learning: Modeling Performance of Configurable Systems. In *ICSE*.

[116] VP9 Website 2021. VP9 Website. https://www.webmproject.org/vp9/.

[117] J. White, B. Dougherty, and D.C. Schmidt. 2009. Selecting Highly Optimal Architectural Feature Sets with Filtered Cartesian Flattening. *Journal of Systems and Software* (Aug. 2009).

[118] J. White, B. Doughtery, and D. Schmidt. 2008. Filtered Cartesian Flattening: An Approximation Technique for Optimally Selecting Features While Adhering to Resource Constraints. In *SPLC*.
[119] Wikipedia. 2016. 68-95-99.7 Rule. https://en.wikipedia.org/wiki/68%E2%80%9395%E2%80%9399.7_rule.
[120] Wikipedia. 2018. Conjunctive Normal Form. https://en.wikipedia.org/wiki/Conjunctive_normal_form.
[121] Wikipedia. 2021. Box Plot. https://en.wikipedia.org/wiki/Box_plot.
[122] Wikipedia. 2021. Integer Programming. https://en.wikipedia.org/wiki/Integer_programming.
[123] Wikipedia. 2021. Random Search. https://en.wikipedia.org/wiki/Random_search.
[124] Wikipedia. 2022. Chain Rule. https://en.wikipedia.org/wiki/Chain_rule.
[125] Wikipedia. 2022. Equisatisfiability. https://en.wikipedia.org/wiki/Equisatisfiability.
[126] Wikipedia. 2022. Order Statistics. https://en.wikipedia.org/wiki/Order_statistic.
[127] Y. Xue and Y. Li. 2018. Multi-Objective Integer Programming Approaches for Solving Optimal Feature Selection Problem. In *ICSE*.
[128] T. Ye and S. Kalyanaraman. 2003. A Recursive Random Search Algorithm for Large-Scale Network Parameter Configuration. *PER* (June 2003).
[129] Y. Zhang, J. Guo, E. Blais, and K. Czarnecki. 2015. Performance Prediction of Configurable Software Systems by Fourier Learning. In *ASE*.
[130] Y. Zhu et al. 2017. BestConfig: Tapping the Performance Potential of Systems Via Automatic Configuration Tuning. In *SoCC*.
[131] M. Zuluaga, G. Sergent, A. Krause, and M. Püschel. 2013. Active Learning for Multi-Objective Optimization. In *PMLR*.

A |ℂ| > 1000: WHEN AN INFINITE SPACE CAN APPROXIMATE A DISCRETE SPACE

|ℂ| is big enough when Eqns (4)-(6) are satisfied, *i.e.,* when the mean ($\overline{c_{1,n}}$) and standard deviation ($\overline{\sigma_{1,n}}$) of many samples converge to their theoretical counterparts, $c_{1,n}$ and $\sigma_{1,n}$, Eqns (4)-(6). Fig. 24 shows the result of simulating 1,000 samples, with |ℂ| configurations each, for different values of |ℂ|. For each |ℂ|, there is one point representing the mean, $\overline{c_{1,n}}$, in Fig. 24a, and one point for the standard deviation, $\overline{\sigma_{1,n}}$, in Fig. 24(b). Red lines show the theoretical $c_{1,n}$ and $\sigma_{1,n}$ counterparts.

The vertical (blue) line of Fig. 24 shows the approximation works well for |ℂ|=1024 (a tiny SPL), *i.e.,* for SPLs with 10 unconstrained optional features. A more conservative estimate was |ℂ|>2000 in [91].

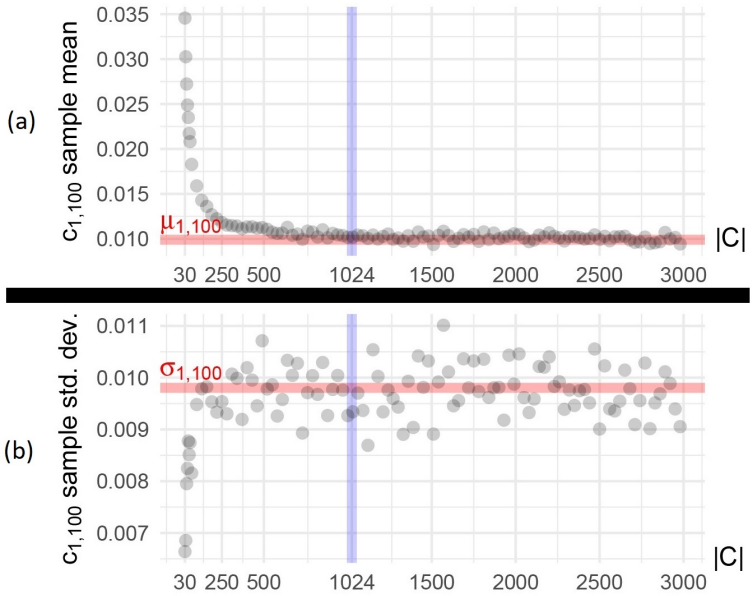

Fig. 24. Minimal |ℂ| to satisfy the URS continuous Approximation.

B PROOF OF UNIFORMITY OF THE URS ALGORITHM

Two kinds of probabilities need to be distinguished to prove the uniformity of Alg. 1:

(1) The probability $\mathtt{P(c)}$ that configuration $\mathtt{c}$ is sampled; and
(2) The probability $\mathtt{P(f)}$ that feature $\mathtt{f}$ belongs to a sampled configuration, i.e., $\mathtt{P(f)} = \frac{|\phi \wedge \mathtt{f}|}{|\phi|}$.

Uniformity means that every configuration has the same chance to be sampled. According to the probability definition, $\sum_{\mathtt{i}=1}^{|\phi|} \mathtt{P(c_i)} = 1$. Hence, uniformity is satisfied whenever $\mathtt{P(c)} = \frac{1}{|\phi|}$ for any $\mathtt{c}$.

Alg. 1 samples a configuration by incrementally assigning true or false to each of the ω features in a feature model. In Eqn (13), $\mathtt{a_i}$ stands for the value assigned to feature $\mathtt{f_i}$. Due to feature constraints, assignments depend on each other, and so feature values must be generated following the *chain rule* [124] to ensure the final configuration is valid, *i.e.,* using feature conditional probabilities, Eqn (14). In each iteration $\mathtt{i}$, the algorithm produces a random assignment $\mathtt{a_i}$ by taking into account the probabilities of the previous assignments $\mathtt{a_1}, \mathtt{a_2}, \ldots, \mathtt{a_{i-1}}$ (Eqn. 15). At the end, all features are assigned and $|\phi \wedge \mathtt{a_1} \wedge \mathtt{a_2} \wedge \ldots \wedge \mathtt{a_\omega}| = 1$, since a complete feature assignment corresponds to a unique configuration. As a result, the probability of sampling the configuration is $\mathtt{P(c)} = \frac{1}{|\phi|}$ (Eqn. 16), which guarantees the sampling procedure is uniform.

$$\mathtt{P(c)} = \mathtt{P}(\mathtt{a_1} \cap \mathtt{a_2} \cap \mathtt{a_3} \cap \ldots \cap \mathtt{a_\omega}) \tag{13}$$

$$= \mathtt{P}(\mathtt{a_1}) \cdot \mathtt{P}(\mathtt{a_2}|\mathtt{a_1}) \cdot \mathtt{P}(\mathtt{a_3}|\mathtt{a_1} \cap \mathtt{a_2}) \cdot \ldots \cdot \mathtt{P}(\mathtt{a_\omega}|\mathtt{a_1} \cap \mathtt{a_2} \cap \mathtt{a_3} \cap \ldots \cap \mathtt{a_{\omega-1}}) \tag{14}$$

$$= \frac{|\phi \wedge \cancel{\mathtt{a_1}}|}{|\phi|} \cdot \frac{|\phi \wedge \cancel{\mathtt{a_1}} \wedge \mathtt{a_2}|}{|\phi \wedge \cancel{\mathtt{a_1}}|} \cdot \frac{|\phi \wedge \cancel{\mathtt{a_1}} \wedge \cancel{\mathtt{a_2}} \wedge \mathtt{a_3}|}{|\phi \wedge \cancel{\mathtt{a_1}} \wedge \cancel{\mathtt{a_2}}|} \cdots \frac{|\phi \wedge \mathtt{a_1} \wedge \mathtt{a_2} \wedge \ldots \wedge \mathtt{a_\omega}|}{|\phi \wedge \cancel{\mathtt{a_1}} \wedge \cancel{\mathtt{a_2}} \wedge \ldots \wedge \mathtt{a_{\omega-1}}|} \tag{15}$$

$$= \frac{1}{|\phi|} \tag{16}$$

C STATISTICAL SIGNIFICANCE

Results of Sections 5 and 6 were analyzed to test their statistical significance. As usual in science, the confidence level was set to 95%.

A result is said to be *statistically significant* when it is unlikely to happen by chance. That is, Sections 5 and 6 answer **RQ1**–**RQ4** by analyzing a sample of SPLs (BerkeleyDBC, 7z, VP9, axTLS, and ToyBox). However, we could have accidentally selected a very particular set of SPLs that does not reflect the characteristics of the whole population of SPLs. Statistical significance means rejecting that possibility, thus supporting the generality of our results.

C.1 RQ1 and RQ2

An ANOVA test is the standard way to check if the differences among each algorithm's $\mathtt{c_{no}}$s in Section 5 were statistically significant [38]. However, our experiments violated ANOVA preconditions:

- $\mathtt{c_{no}}$s for each algorithm were not normally distributed. Table 8 summarizes Shapiro-Wilk tests [99] conducted per algorithm; as all p-values were ≤ 0.05, normality was rejected.
- The variance of $\mathtt{c_{no}}$s returned by each algorithm was highly different. In particular, the Levene test [74] for variance homogeneity produced $\mathtt{F} = 191.5$ and p-value ~ 0. As p-value ≤ 0.05, variance homogeneity was rejected.

The Kruskal-Wallis test [70] was used as the non-parametric alternative to ANOVA. It raised $\mathtt{H}=3.050$ and p-value ~ 0. As p-value ≤ 0.05, the test concluded that at least one of the algorithms achieved $\mathtt{c_{no}}$s significantly different from at least one of the other algorithms.

Algorithm	W	p-value
SRS	0.599	~ 0
RRS	0.238	~ 0
DeepPerf	0.714	~ 0
SPLCon. S1	0.753	~ 0
SPLCon. S2	0.703	~ 0
SPLCon. S3	0.611	~ 0
SPLCon. S4	0.580	~ 0
SPLCon. S5	0.535	~ 0

Table 8. Shapiro-Wilk's

To determine precisely for which algorithms the c_{no}s differ, all pairwise comparisons in Table 9 were performed following the method described in [104]. First, all c_{no}s were ranked (i.e., the smallest c_{no} scored a rank of 1, the second smallest one a rank of 2, and so on). Then, the mean of the c_{no} ranks was computed for each algorithm. The absolute value of the difference between the means of every pair of algorithms was calculated. These absolute values, called *observed differences*, were compared to thresholds, named *critical differences* and calculated from the number of experiments carried out per algorithm and the confidence level.

According to [104], observed differences should be considered statistically significant whenever they are ≥ than their corresponding critical differences. Therefore, all observed differences were statistically significant except when comparing `DeepPerf` to `SPLConqueror S1`, and `SPLConqueror S2` to `SPLConqueror S4`.

To summarize:

- The Kruskal-Wallis and multiple comparison tests support the statistical significance of **RQ1** (Section 5.2).
- Levene test supports the statistical significance of **RQ2** (Section 5.3).

Comparison	Observed difference	Critical difference	Statistically significant?
SRS *vs.* RRS	1938.758	293.0368	yes
SRS *vs.* DeepPerf	2398.176	306.424	yes
SRS *vs.* SPLCon. S1	2094.880	350.495	yes
SRS *vs.* SPLCon. S2	1491.906	350.495	yes
SRS *vs.* SPLCon. S3	522.209	350.495	yes
SRS *vs.* SPLCon. S4	1230.784	350.495	yes
SRS *vs.* SPLCon. S5	811.818	350.495	yes
RRS *vs.* DeepPerf	4336.934	293.037	yes
RRS *vs.* SPLCon. S1	4033.646	338.854	yes
RRS *vs.* SPLCon. S2	3430.664	338.854	yes
RRS *vs.* SPLCon. S3	2460.968	338.854	yes
RRS *vs.* SPLCon. S4	3169.542	338.854	yes
RRS *vs.* SPLCon. S5	1126.934	338.854	yes
DeepPerf *vs.* SPLCon. S1	303.288	350.495	no
DeepPerf *vs.* SPLCon. S2	906.270	350.495	yes
DeepPerf *vs.* SPLCon. S3	1875.966	350.495	yes
DeepPerf *vs.* SPLCon. S4	1167.391	350.495	yes
DeepPerf *vs.* SPLCon. S5	3209.994	350.495	yes
SPLCon. S1 *vs.* SPLCon. S2	602.982	389.613	yes
SPLCon. S1 *vs.* SPLCon. S3	1572.678	389.613	yes
SPLCon. S1 *vs.* SPLCon. S4	864.104	389.613	yes
SPLCon. S1 *vs.* SPLCon. S5	2906.707	389.613	yes
SPLCon. S2 *vs.* SPLCon. S3	969.696	389.613	yes
SPLCon. S2 *vs.* SPLCon. S4	261.122	389.613	no
SPLCon. S2 *vs.* SPLCon. S5	2303.724	389.613	yes
SPLCon. S3 *vs.* SPLCon. S4	708.574	389.613	yes
SPLCon. S3 *vs.* SPLCon. S5	1334.028	389.613	yes
SPLCon. S4 *vs.* SPLCon. S5	2042.603	389.613	yes

Table 9. Multiple comparison test.

C.2 RQ3

Table 10 summarizes the significance of the correlations between `MAPE` and β reported in Table 6 (Section 5.4). As all p-values ≤`0.05`, all correlation measures were statistically significant.

C.3 RQ4

Analogous to Appendix C.1, a `t-test` would be the standard way [38] to check the significance of the `SRS` and `RRS` difference reported in Section 6; however, the experimental data violated `t-test` preconditions:

- The build sizes of the configurations obtained with `SRS` and `RRS` were not normally distributed. Table 11 summarizes Shapiro-Wilk tests [99] conducted per algorithm; as all p-values were ≤`0.05`, normality was rejected.
- The build size variance for each algorithm was heterogeneous. The Levene test [74] produced `F=28.453` and p-value=$1.46 \cdot 10^{-7}$. As p-value ≤`0.05`, variance homogeneity was rejected.

The Mann-Whitney U-test [38], also known as Wilcoxon signed-rank test, was used as the non-parametric alternative to `t-test`. It raised `W=46043` and p-value~`0`. As p-value ≤`0.05`, the test concluded that `SRS` and `RRS` difference was statistically significant.

Algorithm	p-value			
	Spearman's ρ	Kendall's τ	Hoeffding's D	dCor
DeepPerf	$2.908 \cdot 10^{-6}$	$3.198 \cdot 10^{-6}$	~ 0	~ 0
SPLCon. S1	$8.591 \cdot 10^{-11}$	$1.650 \cdot 10^{-8}$	~ 0	~ 0
SPLCon. S2	~ 0	~ 0	~ 0	~ 0
SPLCon. S3	~ 0	~ 0	~ 0	~ 0
SPLCon. S4	~ 0	~ 0	~ 0	~ 0
SPLCon. S5	~ 0	~ 0	~ 0	~ 0

Table 10. Significance tests of MAPE and β correlation.

Algorithm	W	p-value
SRS	0.829	~ 0
RRS	0.741	~ 0

Table 11. Shapiro-Wilk's normality tests for t-test.

D PROPOSITIONAL FORMULA ϕ TO CNF CONVERSION

SAT and #SAT solvers require a *Conjunctive Normal Form* (CNF) formula as input [20, 120]. Transforming ϕ into a CNF formula ϕ^{cnf} is straightforward with rules of logical equivalence. But doing so may increase the number of clauses exponentially [120] and simplifying ϕ^{cnf} to reduce the number of clauses is nontrivial [63, 86].

To avoid this, *Equisatisfiable Transformations* (ETs) are used. Two formulas are *equisatisfiable* when one formula is satisfiable only if the other is satisfiable, and vice versa [125]. ETs produce a CNF formula ϕ^{cnf} that is equisatisfiable to ϕ [113]. There are many ETs [58, 96, 113] not all of which are suitable for URS.

Consider: $\phi = (a \wedge b) \vee (c \wedge d)$. An ET from Plaisted and Greenbaum [96] introduces additional variables x_1 and x_2 for the clauses of ϕ:

$$\phi^{cnf} = (x_1 \vee x_2) \wedge (\neg x_1 \vee a) \wedge (\neg x_1 \vee b) \wedge (\neg x_2 \vee c) \wedge (\neg x_2 \vee d)$$

Each row of Table 12 is a solution of both ϕ and ϕ^{cnf}. The last solution of ϕ corresponds to 3 solutions of ϕ^{cnf}. A problem for URS is exposed: using ϕ^{cnf} yields a ***biased*** sampling of ϕ. Statistical predictions by URS of ϕ^{cnf} are distorted predictions about ϕ:

- $|\phi^{cnf}|$ is 9 and $|\phi|$ is 7, a 28% over-estimation; and
- The percentage of products with feature d in ϕ^{cnf} is $78\%=\frac{7}{9}$, whereas the correct answer in ϕ is $71\%=\frac{5}{7}$, a 10% over-estimation.

ϕ				ϕ^{cnf}					
a	b	c	d	a	b	c	d	x_1	x_2
1	1	0	0	1	1	0	0	1	0
1	1	0	1	1	1	0	1	1	0
1	1	1	0	1	1	1	0	1	0
0	0	1	1	0	0	1	1	0	1
0	1	1	1	0	1	1	1	0	1
1	0	1	1	1	0	1	1	0	1
1	1	1	1	1	1	1	1	1	0
				1	1	1	1	0	1
				1	1	1	1	1	1

Table 12. Solution Comparison Between ϕ and ϕ^{cnf}.

How do redundant solutions arise? We observed empirically that if ϕ^{cnf} adds *no* new variables to ϕ then all is OK: URS statistics about ϕ^{cnf} match ϕ because $|\phi^{cnf}|=|\phi|$.

Adding variables *might not be* a problem. Tseitin's transformation [113], a well-known ET method, adds variables but does *not* increase the number of solutions. Tseitin's transformation extends the Plaisted and Greenbaum transformation with blocked clauses [71]. The elimination of blocked clauses [61], which is a SAT preprocessing technique used in top-tier solvers, removes those clauses and introduces redundant solutions.

The example of Table 12 shows there are bad ETs that both add variables *and* distort statistical predictions. The pragmatic problem is this: ***Given a feature-model-to-propositional-formula tool, you may not know if the tool (nor the #SAT solver that uses the propositional formula) employs bad ETs if extra variables are used.***

We used the Kmax tool [39] in our work which avoids translation controversies as it adds no extra variables in translating ϕ to ϕ^{cnf}.

Also, *Projected Model Counters* (#∃SAT) [12] can be used as an alternative to classical #SAT solvers to prevent miscounting. #∃SAT counts the solutions of ϕ^{cnf} with respect to an input set of relevant variables, called *projection variables*. If all variables in ϕ are specified as projection variables, #∃SAT

will ignore any other auxiliary variables in ϕ^{cnf}, thus computing the right count. Further, sampling with BDDs avoids ET problems as BDDs don't require the input formula to be in any particular form. This is an advantage of using BDDs.